ASSESSING REMOTE SENSING APPLICATION ON RANGELAND INSURANCE IN CANADIAN PRAIRIES

A Thesis Submitted to the
College of Graduate Studies and Research
in Partial Fulfillment of the Requirements
for the Degree of Master of Science
in the Department of Geography
University of Saskatchewan
Saskatoon

By

Weidong Zhou

Permission to use

In presenting this thesis in partial fulfillment of the requirements for a Postgraduate degree from the University of Saskatchewan, I agree that the Libraries of this University may make it freely available for inspection. I further agree that permission for copying of this thesis in any manner, in whole or part, for scholarly purposes may be granted by the professor who supervised my thesis work or, in their absence, by the Head of the Department or the Dean of the College in which my thesis work was done. It is understood that any copying, publication, or use of this thesis or parts thereof for financial gain shall not be allowed without my written permission. It is also understood that due recognition shall be given to me and the University of Saskatchewan in any scholarly use which may be made of any material in my thesis.

Requests for permission to copy or to make other use of material in this thesis in whole or part should be addressed to:

Head of the Department of Geography
University of Saskatchewan
Saskatoon, Saskatchewan, S7N 5A5

Abstract

Part of the problem with implementing a rangeland insurance program is that the acreage of different pasture types, which is required in order to determine an indemnity payment, is difficult to measure on the ground over large areas. Remote sensing techniques provide a potential solution to this problem. This study applied single-date SPOT (Satellite Pour I'Observation de la Terre) imagery, field collected data, and geographic information system (GIS) data to study the classification of land cover and vegetation at species level. Two topographic correction models, Minnaert model and C-correction, and two classifying algorithms, maximum likelihood classifier (MLC) and artificial neural network (ANN), were evaluated. The feasibility of discriminating invasive crested wheatgrass from natives was investigated, and an exponential normalized difference vegetation index (ExpNDMI) was developed to increase the separability between crested wheatgrass and natives. Spectral separability index (SSI) was used to select proper bands and vegetation indices for classification. The results show that topographic corrections can be effective to reduce intra-class rediometric variation caused by topographic effect in the study area and improve the classification. An overall accuracy of 90.5% was obtained by MLC using Minnaert model corrected reflectance, and MLC obtained higher classification accuracy (~5%) than back-propagation based ANN. Topographic correction can reduce intra-class variation and improve classification accuracy at about 4% comparing to the original reflectance. The crested wheatgrass was over-estimated in this study, and the result indicated that single-date SPOT 5 image could not classify crested wheatgrass with satisfactory accuracy. However, the proposed ExpNDMI can reduce intra-class variation and enlarge inter-class variation, further, improve the ability to discriminate invasive crested wheatgrass from natives at 4% of overall accuracy. This study revealed that single-date SPOT image may perform an effective classification on land cover, and will provide a useful tool to update the land cover information in order to implement a rangeland insurance program.

Acknowledgements

There are many people that supported this research. First, I would like to thank Dr. Xulin Guo, my thesis supervisor. She provided the opportunity, environment and financial support to make my research project possible, as well as guidance and encouragement throughout the entire project. I would also like to thank other members of my masters committee, Dr. Abraham Akkerman and Dr. Seifu Gebremeskel Guangul, and the external examiner, Dr. Xianhua Kong, for their guidance and support through my master study. They provided valuable suggestions that improved this work.

I gratefully acknowledge Chunhua Zhang, Yuhong He, Tara Dupuis, and Selena Black for their assistance in field data collection. I appreciate their generous help in providing time and advice whenever I needed help. I am also thankful to Grasslands National Park for the support in the field data collection.

Financial support for this research provided by the following grants was greatly appreciated: Agricultural Financial Service Corporation, Alberta, Canada (AFSC) and the Department of Geography at the University of Saskatchewan.

Reaching this goal would not have been possible without the encouragement and support from my wife and daughter, my parents, and my relatives.

Table of contents

List of tables

List of figures

List of abbreviations

AFSC	Agricultural Financial Service Corporation, Alberta, Canada
ANN	Artificial Neural Network
ATSAVI	Adjusted Transformed Soil-Adjusted Vegetation Index
AVHRR	Advanced Very High Resolution Radiometer
AVIRIS	Airborne Visible/Infrared Imaging Spectrometer
BP	Back-Propagation
BRDF	Bidirectional Reflectance Distribution Function
CASI	Compact Airborne Spectrographic Imager
DEM	Digital Elevation Model
DN	Digital Number of the image
DTC	Decision Tree Classifier
DTM	Digital Terrain Model
ESUN	Mean Solar Exoatmospheric Irradiances
ExpNDMI	Exponential NDMI
GCP	Ground Control Point
GIS	Geographic Information System
GNP	Grasslands National Park of Canada
GPS	Global Positioning System
HRV	High Resolution Visible
IL	Illumination
LAI	Leaf Area Index
M	Minnaert
MIR	Middle Infrared
MLC	Maximum Likelihood Classifier
MSAVI	Modified Soil Adjusted Vegetation Index
NDMI	Normalized Difference Vegetation Index

NDVI	Normalized Difference Vegetation Index
NIR	Near Infrared
NOAA	National Oceanic and Atmospheric Administration
PFRA	Prairie Farm Rehabilitation Administration, Agriculture and Agri-Food Canada
RMSE	Root Mean Square Error
SAVI	Soil Adjusted Vegetation Index
SD	Standard Deviation
SPOT	Satellite Pour I'Observation de la Terre (France)
SR	Simple Ratio (vegetation index)
SSI	Spectral Separability Index
TM	Thematic Mapper (Landsat)
TSAVI	Transformed Soil-Adjusted Vegetation Index
TVI	Triangular Vegetation Index
UTM	Universal Transverse Mercator (projection)
VI	Vegetation Index

Chapter 1 Introduction

1.1 Difficulties with rangeland insurance

As one of the components of a global ecosystem, grasslands have important commercial, aesthetical, and environmental functions in providing livestock forage, wildlife habitat, recreational opportunities, carbon sinks, and reservoirs of plant and animal genes**.** However, grasslands are now confronted with the most significant environmental challenges from climate change, and we are already seeing the effects of such change in Canada (Guo et al., 2004; Adams et al., 1998). Climate change is expected to influence crop and livestock production, hydrologic balances and other components of agricultural systems. For example, crop and livestock yields are directly affected by changes in climatic factors such as temperature, precipitation, and the frequency and severity of extreme events like droughts, floods, and wind storms (Karoly et al., 2003). Drought is one of the most serious difficulties farmers/ranchers face in maintaining a business on the land. In Alberta, Canada, the 2002 crop year was the worst year in history for crop losses resulting from severe widespread drought in the province, and claims under crop insurance were as high as $804 million (AFSC, 2003). In the United States, drought costs on average around 6–8 billion dollars annually, while the average yearly cost of floods and hurricanes is 2.41 billion and 1.2 – 4.8 billion dollars, respectively. In 1988, the drought struck a large part of the United States, and the original economic loss estimate for this drought was $39.4 billion (Hayes et al., 2004).

One mitigation solution to this problem comes through various crop/rangeland insurance programs. According to The Crop Insurance Act (C-47.2, 2003) of Saskatchewan, crop insurance means:

> (i) insurance against loss of an insured crop caused by drought, flood, hail, wind, frost, lightning, excessive rain, snow, hurricane, tornado, wildlife, accidental fire, insect infestation, plant disease or any other peril designated in the regulations; and (ii) insurance against the occurrence or non-occurrence of any climatic event designated in the regulations that has the potential to cause loss to an insurable crop.

In a typical crop/rangeland insurance program, the rancher pays a premium based on the insured rangeland acreage of different pasture types, and the annual yield of different pasture types is estimated at the end of the growing season. This yield estimate is then compared to a historical average of corresponding pasture type. If yield falls below the coverage level purchased at a certain threshold, then an indemnity payment will go to the insured rancher. Rangeland and pasture, however, are different from traditionally insured crops. The grass is not harvested and measured directly, as is the case with corn, wheat, or cotton, but is instead eaten by grazing animals. The grass yield for a growing season is therefore difficult to calculate by traditional approaches over large areas, such as ground surveys (Rowley, 2002).

Another problem is from the identification of acreage and distribution for different pasture types in a rangeland insurance program. The information of land cover/pasture type is used by insurance companies to verify the pasture types and acreage the ranchers applied for participating in a rangeland insurance program in order to combat insurance fraud and abuse, assist in evaluating the regions impacted by climate change, and provide the background for local adjustment of insurance (Goodwin et al., 2004). The information is also used as the basis of yield calculation and comparison with the historical average. In addition, increased participation in insurance programs provokes statistically significant acreage responses. Acreage effects brought about by participation in rangeland insurance programs could affect insurance prices and thus have important policy implications. Land cover information is necessary to assess the potential of

acreage effects (LaFrance et al., 2002). The information of land cover that insurance companies used usually comes from existing land cover/land use data, however, it may be unreliable (because of the lower accuracy), obsolete (because land cover changes from year to year with climate change and human activities), or may not meet the requirements for a rangeland insurance program. For example, the information of land cover that Agricultural Financial Service Corporation (AFSC), Alberta, Canada used was from the land cover map developed by Prairie Farm Rehabilitation Administration (PFRA) using Landsat imagery (resolution 30 m) and computerized classification techniques from 1995 to 1997 (AFSC, 2002). On this map, nine broad land cover classes were classified, but there are no subclasses for grassland. Therefore, it could not meet the requirements for pasture type information needed in the insurance program, and may also not reflect the situation of the current land cover. Moreover, the accuracy of this map is not reliable; its accuracy was only verified using the 1996 Statistics Canada census data and the original imagery, while the resolution of Statistics Canada census data was as coarse as 1.0 km (PFRA, 2001). Therefore, it can be problematic to use PFRA land cover map in AFSC's insurance program. However, it is difficult, if not impossible, to update the land cover information using ground surveys. Mapping land cover based on field data is time-consuming, subjective, error-prone, and economically inefficient for large areas.

The two measurements, grass yield and acreage of different pasture types, become therefore the key problems in implementing a rangeland insurance program. In order for a rangeland and pasture insurance program to be technologically feasible and effectively implemented, it needs to solve the two key problems. However, this research limited its focus on exploring the effective methods to update the land cover/pasture type data in order to meet the requirements for land cover/pasture type information in implementing a rangeland insurance program. Hereinafter, the discussion centers on the issues related

to rangeland/land cover classification.

1.2 Applications of remote sensing in land cover/species classification

Remote sensing techniques provide a potential solution to the problem of updating the land cover/pasture type information (ASFC, 2002). The strength of satellite remote sensing for land cover mapping is in the low cost per unit of land area associated with data capture and image analysis as well as the ability to easily and repeatedly acquire data over geographically isolated areas. In the past years, satellite imagery has been widely used on vegetation/land cover classification, and a numerous studies on land cover/vegetation classification using remotely sensed data have been conducted (Cingolan et al., 2004; Erbek et al., 2004; Bruzzone et al., 2002; Langley et al., 2001; Underwood et al., 2003).

Algorithm is a central issue in classification of remote sensing imagery. There are a variety of classification algorithms applied to separate remotely sensed data into meaningful groups or classes. Classification algorithms are usually divided in two categories, supervised and unsupervised methods. Supervised methods have on the overall produced higher accuracies than unsupervised methods; however, they require a user's interaction to determine classes and characterize them in the training process (Miguel-Ayanz et al., 1997). The conventional supervised classification algorithms, such as parallelpiped, maximum likelihood classifier (MLC), and minimum distance, are still applied at present **(**Qiu et al., 2004; Franklin et al., 2001). Some newly developed algorithms, such as decision tree classifier (DTC) and artificial neural netwoks (ANNs), have become popular in recent years. Assessment of such newly developed algorithms has found them to be superior to conventional algorithms (Michelson, 2000). However, the major obstacle for using remote sensing data for land cover mapping is the difficulty in consistently interpreting surface spectral characteristics under a wide range of

environmental conditions. Each algorithm encounters specific drawbacks, and is not applicable in all ecosystems (McIver et al., 2002; Sommer et al., 1998). Therefore, these algorithms, whether conventional or newly developed, remain to be evaluated in practical applications using operational satellite data (Michelson, 2000).

Choice of spatial resolution is another key issue in remote sensing land cover classification. Until recently, satellite data have generally offered only two options for regional-scale analyses: images with coarse-resolution, such as the advanced very high resolution radiometer (AVHRR; Hansen et al., 2000) and SPOT Vegetation (Malingreau et al., 1995; Mayaux et al., 1998), and high resolution data from sensors such as Landsat and SPOT HRV (Chomentowski et al., 1994; Wessels et al., 2004; Tucker et al., 2000). The former has the advantage of high, daily temporal resolution but the disadvantage of coarse spatial resolution of 1 km or greater, which introduces significant difficulties with mixed pixels and means that most pixels will be made up of a diversity of land cover classes. The latter, high resolution data have the advantage of high spatial resolution (15–30 m), but infrequent temporal resolution. Limited acquisitions from the Landsat and SPOT sensors pose challenges to historical and multitemporal analyses. Higher spatial resolution data usually can produce higher classification accuracy and more detailed land cover classes. New generation of satellite images with high resolution (<1 m, such as IKONOS and Quickbird) can get reasonable classification accuracy (Cochrane, 2000). However, when using high resolution imagery, it requires a significant amount of data to cover the entire study area; hence the data volume may become too large for a timely and efficient analysis. Moreover, it is expensive to obtain high resolution data (Cochrane, 2000).

It is demonstrated that broad land cover classes can sometimes be satisfactorily classified at a local level with single-date images. However, the similarity in spectral

reflectance properties of natural surfaces impedes consistent identification and separating of some land cover classes, such as agricultural crops and natural vegetation. In addition, the spectral confusion between land cover classes varies between different seasons: classes which appear quite similar in spring may become separable at earlier or later stages of summer. It is therefore expected that multi-temporal approaches, implying repeated satellite observations at different dates, will provide the means for obtaining more detailed results at regional levels (Sommer et al., 1998). For example, temporal sequences of NOAA AVHRR NDVI may be used to characterize land cover of ecoregions (Ramsey et al., 1995) down to the level of different grass and shrub communities (Kremer et al., 1993). This discrimination is based on differences in phenological patterns of NDVI (normalized difference vegetation index) over single season or several years. Analysis of the Great Plains (USA) grasslands with the use of NDVI based metrics provides evidence that ecologically meaningful land cover classes can be derived for grasslands and pastures by using a temporal NDVI series (Paruelo et al., 1995; Tieszen et al., 1997). However, the optimal cloud-free multitemporal images from different years or seasons are frequently not available and it is difficult to co-register for multi-date image. Also, phenology is influenced by many factors (Ju et al., 2005)), and it is not always reliable to apply multi-temporal approaches in land cover classification.

Digital images taken from mountainous regions often contain a radiometric distortion known as topographic effect. This effect, resulting from the illumination differences due to the angle of the sun and the terrain, causes a variation of image brightness values and is a constraint to an automated classification method (Colby, 1991). The effect of topography on remotely sensed data has been explored by many researchers (Conese et al., 1993; Song, 2003; Feng et al., 2003; Sandmeier et al., 1997) who have attempted to model and reduce the influence of local terrain slope and aspect with the aim of

improving land cover identification. However, these studies have only been carried out on satellite imagery in mountainous areas. Topography effect on spectral response has not been investigated on gently rolling mixed grassland, while it can influence the spectral responses of land covers, and, further, impact the classification accuracy (Soenen et al., 2005; Hejmanowska, 1998; Liu et al., 2005).

Remotely sensed data have also been used to discriminate among grassland species, such as hoary cress, leafy spurge, Brazilian pepper, spotted knapweed, and yellow starthistle (Lauver et al., 1993; Mundt et al., 2005; O'Neill et al., 2000; Lass et al., 2004; Lass et al., 2002; Lass et al., 2000). Many studies applied hyperspectral and multispectral images, such as AVIRIS (Airborne Visible/Infrared Imaging Spectrometer), CASI (Compact Airborne Spectrographic Imager), TM (Thematic Mapper), and SPOT, in separating plants at species level and obtained satisfactory results (Underwood et al., 2003; O'Neill et al., 2000; Lass et al., 2004; Bostater et al., 2004). Glenn et al. (2005) used HyMap hyperspectral data with a resolution of 3.5 m to detect leafy spurge, and the result showed that high resolution hyperspectral imagery can provide high accuracy. Most researchers have applied phenological and vegetation index approaches to distinguish plant species using multitemporal data and obtained satisfactory accuracy (Peterson et al., 2005; Underwood et al., 2003; Egbert et al., 1997; Byeungwoo et al., 1999; Liu et al., 2002; Lass et al., 2005). The new generation of satellite images with high spatial resolution (e.g., IKONOS and Quirkbird) can greatly advance plant detection at species level (Fuller, 2005). However, the principal challenge in using remote sensors to separate plant species lies in the spectral similarity across species and the mixing of different species. Therefore, accurate classification at species level is still difficult (Lawrence et al., 2006).

1.3 Applications of remote sensing in rangeland insurance

Several studies have been carried out to apply remote sensing techniques in rangeland insurance (Rowley, 2002; AFSC, 2003). AFSC (2001) applied Landsat conducted classification map as a 'mask' to remove all the non-pasture area in their program, so that the satellite imagery insurance program only uses the region of pasture land to calculate the payment. A pilot insurance program for assessing production of native pasture and determining payments using satellite imagery (MODIS and AVHRR NDVI composites) was introduced in 2001 in the areas of southern Alberta, Canada. This three-year project investigated the feasibility of estimating pasture growth in the current year, which was then compared with an estimate of normal pasture growth from previous years (AVHRR historical database). The program was limited to a small area until enough information was gathered to determine the viability of the program (AFSC, 2005). In the United States, Watts and Associates, Inc. (W&A) and Terra Metrics Agriculture, Inc. (TMAI) used satellite imagery in the insurance program to identify and map various types and characteristics of grasslands and agricultural land features (Atwood et al., 2005). The results showed that remote sensing was a useful tool in implementing a rangeland insurance program.

1.4 Research gaps and questions

Most of the applications of remote sensing in rangeland insurance, however, are still at research stage or in trial, and have difficulties in dealing with the classification for pasture types. Currently, there is no standardized approach available to address this issue, and unsatisfactory accuracy of classification is still a critical issue with remote sensing in implementing a rangeland insurance program, especially at species level (Langley et al., 2001). Uncertainty of classification varies with the methodologies and ecosystems (McIver et al., 2002). Traditional classification methods, such as maximum likelihood

classifier (MLC), and newly developed methods, such as decision tree classifier (DTC) and artificial neural networks (ANNs), still have substantial disadvantages in practical use. MLC is limited by the assumptions about the probability distribution of features; DTC highly depends on the analyst's expertise and knowledge; and ANNs have the uncertainty of how many layers and neurons are enough. Apart from classification algorithms, remote sensing classification is more impacted by many other factors, such as the nature of the sensor, environmental conditions (e.g., terrain), quality of the training data, and the applicability of target classes. Spectral transformation methods, such as topographic correction and vegetation indices (VIs), have been widely applied in classification and obtained better results. However, applications of these methods vary greatly with the different ecosystems and remotely sensed datasets, and no universal pattern or procedure can be expected to exist (McIver et al., 2002).

Limitations with current remote sensing classification methods on pasture hamper the implementing of the rangeland insurance program. Therefore, further research is still required to improve the remote sensing classification of land cover/pasture type on mixed grassland for implementing a rangeland insurance program.

The shortcomings with respect to the application of remote sensing on land cover classification mentioned above raise many questions for rangeland insurance program implementation:

● Can the topographic corrections reduce spectral variations within land cover classes and improve the classification on gently rolling mixed grassland?

● What remote sensing classification approach can be effective to separate the different land covers on the arid mixed grassland? and

● Can the single-date remotely sensed image with medium resolution discriminate vegetation at species level?

1.5 Objectives

The overall purpose of this study is to develop an effective remote sensing approach for updating the land cover information in order to effectively implement a rangeland insurance program, and improve the accuracy of remote sensing classification for land cover/pasture species on mixed grassland with medium resolution data. This research was in conjunction with the AFSC's rangeland insurance research project, which was to be conducted in Grassland National Park of Canada, southern Saskatchewan. AFSC has been operating a satellite program in Alberta since 2001 and attempting to expand the area currently offering this insurance product by using higher resolution imagery. The information that was used to determine pasture acreages is based on a land cover classification that was done by PFRA using Landsat imagery from 1995 to 1997. However, it may not accurately reflect the current land cover. The objective of this research project was to investigate methods on accurate land cover classification with the use of higher resolution satellite imageries in order to reduce the uncertainty of rangeland insurance, and develop a province-wide pasture insurance tool using a remote sensing approach.

A review of remote sensing studies in land cover classification revealed that, in addition to the regular problems encountered in land cover classification (i.e., atmospheric effect, the date of image acquisition, and high heterogeneous land cover), the effects of topography, and applicability of classifying algorithm can impact the accurate identification of land cover. The specific objectives of this research are: (1) to evaluate the effectiveness of different topographic corrections in reducing spectral variation among interested land cover classes and improving the classification accuracy on gently rolling mixed grassland; (2) to explore the effective remote sensing classification methods to separate other land cover on mixed grassland in order to reduce the

uncertainty in implementing a rangeland insurance program; and (3) to investigate the unique spectral feature of invasive species (crested wheatgrass) and discriminate it from native grasslands based on vegetation indices using single-date images.

Chapter 2 Study area and remote sensing data preprocessing

2.1 Study area

The study area, Grasslands National Park of Canada (GNP), is located in southwestern Saskatchewan near the international border of Canada and United States. The two separate blocks that comprise the park and cover approximately 906.5 sq. km. lie between the villages of Val Marie and Killdeer (Figure 2-1). This study limited its focus on west block of GNP and surrounding pastures.

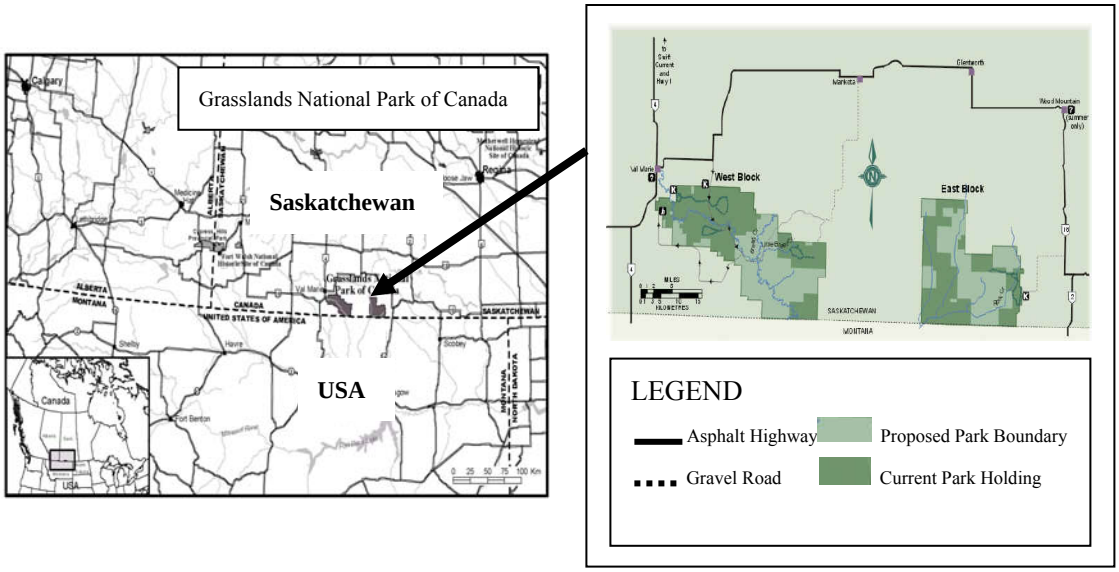

Figure 2-1 Location of Grasslands National Park of Canada.

The park is characterized by gently rolling hills, coulees, badlands, and wide-open spaces, with wide areas of grasslands. The elevation varies from 740 m to 1000 m in this area, and the average elevation is about 860 m. “Mixed-grass prairie” best describes the particular type of grassland associated with the region. The dominant vegetation species include needle-and-thread grass, blue grama, June grass, sagebrush, greasewood, prickly

pear, cactus, creeping juniper, western wheatgrass**,** rose, buckbrush, shrubby cinquefoil, thorny buffalo berry, willow, dry land sedges, spikemoss and lichens. The dominant soil type is a nutrient poor, shallow, clay-loam brown soil. The climate in the park is characterized by semi-arid, short, hot summers and long, cold winters. The total annual precipitation averages 325 mm. Approximately one-third of this total (110 mm) falls as snow, while the remainder (215 mm) falls as rain (GNP, 1997).

Grasslands National Park is the first national park of Canada to preserve a portion of the mixed prairie grasslands, which serves as an in situ gene pool to protect part of the biodiversity of the planet. However, the park has also experienced impact from invasive plants. At least 24 non-native plant species have been reported in the park, most of which are either weedy species associated with surrounding agriculture, or species that have been seeded within the boundary of the Park for agricultural purposes (Peniuk, 1998). One of the major invasive species, crested wheat grass, is of concern because it is used as hay/pasture species and continues to dominate the areas where they were seeded. The potential impacts of crested wheatgrass on park resources and adjacent lands include displacement of native species, interference with the function of natural ecosystems, reduction of native plant populations and biodiversity, and decrease of wildlife habitat quality and total plant cover (Peniuk, 1998).

Although the dominant type of land cover in the park is grassland, there are still large areas of ploughed soil. Of the park land acquired to date, 1.2% (522.2 ha) continues to be cultivated for the production of cereal crops. Agriculture is one of the most important economic activities in this region as well as the main stressor for the conservation of this ecological region. In an area of approximately 16,800 sq. km around the park, approximately 63% of the land is uncultivated. Much of the uncultivated land is native prairie and clustered around the park. However, large areas around the park have been

plowed in the past years. The conversion of prairie to cropland reduces the amount of habitat, and may fragment what is left, for many prairie species (GNP, 1997).

The reasons for selecting GNP as study area include: 1) AFSC's rangeland insurance research program was to be conducted in GNP, and this study was in conjunction with this program; 2) the park represents the typical mixed grassland in prairies; and 3) many remote sensing researches on the grasslands have been carried out in this park, and some continuous observation sites have been established for years and some historical field data are available for this research.

2.2 Remote sensing data acquisition and preprocessing

A cloud-free SPOT image (June 22, 2005) was used in this study for topographic correction and classification test of land cover, which covers the west block of GNP and surrounding pastures (Figure 2-2). The image has 4 bands (Green, Red, NIR, and MIR) with a spatial resolution of 20 m, a solar azimuth of 162.9 degree, and a solar zenith of 26.5 degree. The SPOT satellite imagery was georectified to a universal transverse Mercator (UTM) projection in order to match the field data. Over 30 ground control points (GCPs) and digital elevation model (DEM) were used to correct distortions in raw images with satellite orbital modelling in order to increase the correction accuracy. DEM was used to do the orthorectification. The root mean square error (RMSE) of the registration was controlled to be less than half a pixel.

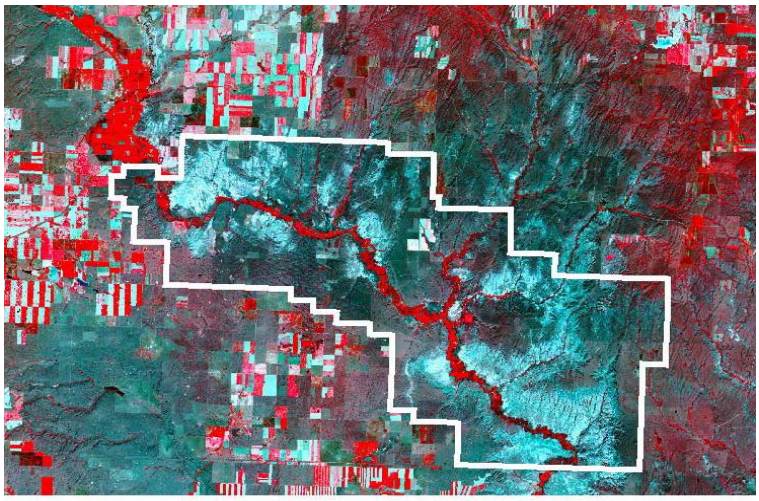

Figure 2-2 SPOT false colour composite for west block of GNP (RGB-NIR, Red, Green).

Varying atmospheric conditions (e.g., meteorological situation), differences in the sun geometry (sun zenith and azimuth angles), and topographic effects strongly influence the true spectral behavior of the ground feather. Each image has to go through a preprocessing step of correcting atmospheric effects before classification can be applied.

Atmosphere is a primary source of noise to accurate measurement of surface reflectance with remote sensing. The influence of the atmosphere degradation was removed and the digital number (DN) of the image was converted to reflectance by the radiometric correction.

Equation (2-1) was used to convert DN to radiance L for all bands:

$$L = a_0 + a_1 * DN \qquad (2\text{-}1)$$

Where a_0 and a_1 are the offset and gain, and they can be obtained from the header file of the imagery. Each band has different offset and gain. Then the radiance was converted to reflectance using equation (2-2) for all bands:

$$\rho_P = \frac{\pi * L_\lambda * d^2}{ESUN_\lambda \cos\theta_s} \quad (2\text{-}2)$$

Where ρ_P is the reflectance, L_λ is the radiance, d is the Earth-Sun distance in astronomical units, $ESUN_\lambda$ is the mean solar exoatmospheric irradiances, and θ_s is the solar zenith angle in degrees.

A large geographic information system (GIS) database was obtained for the Grasslands National Park (GNP). The dataset coverage closely related to this proposed project include contour lines, land use in 1955 and 1982, vegetation types, location of ranch sites, soil cover, hydrology, river and stream systems, surface geology, and critical wildlife habitat. The contour lines with 25 feet interval was used to develop DEM and digital terrain model (DTM, Figure 2-3), which were applied in geometric correction and topographic correction of reflectance.

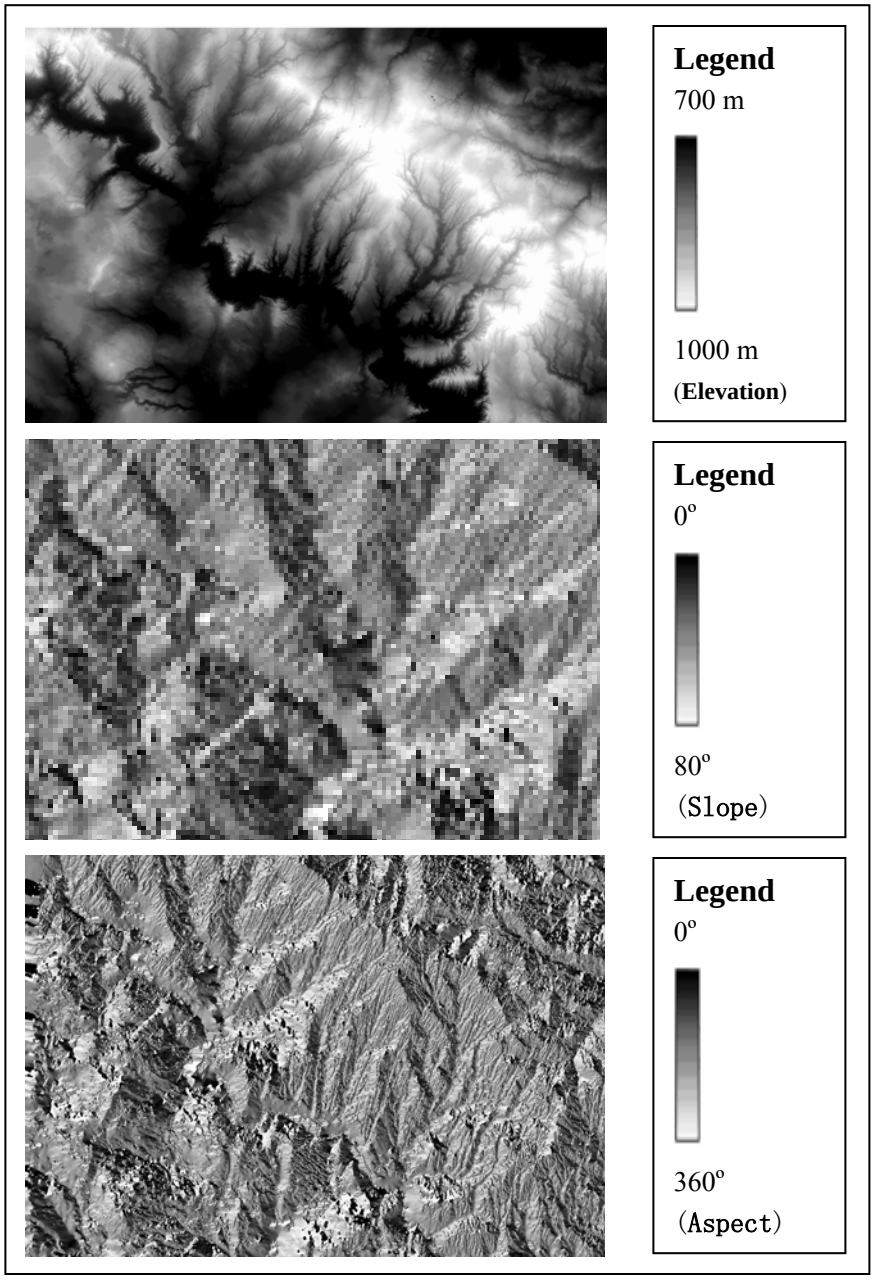

Figure 2-3 DEM and DTM for GNP generated from contour lines.

DEM is used to calculate the surface normal directions (the combination of slopes and aspects), and is the core of the topographic correction processing. A digital contour map of GNP and surrounding areas was used as a source of height information. DEM and

DTM of slope and aspect with a resolution of 20m x 20m were created using ArcGIS9.0 (Figure 2-3), which were applied in the orthorectification and topographic correction algorithms.

2.3 Classification scheme

Prior to collecting training sites, land cover classes were defined. A land cover classification system applied in remote sensing should be ecologically meaningful, useful for land management or specific purposes (e.g., rangeland insurance), and be effectively employed using remote sensor data to obtain certain accuracy (Cingolani, et al., 2004). In this study, six classes of land cover were adopted based on the knowledge gained in earlier studies. The number of classes was decided upon by taking PFRA land cover system into consideration. The PFRA land cover was mapped from Landsat imagery at 30 m resolution in the mid-1990s with nine broad classes (cropland, forage, grassland, shrubland, forest, wetland, badland, water, built-up and other). Table 2-1 lists the six classes, which are major types of land cover in GNP and surrounding areas, and may be detectable by using the satellite data.

Table 2-1 Land cover classification scheme for this study.

Land cover class	Description
Grasslands	Herbaceous cover, closed-open Lands with herbaceous types of cover. Tree and shrub cover is less than 10%.
Croplands	Cultivated and managed areas covered with temporary crops followed by harvest and a bare soil period (e.g., single and multiple cropping systems).
Fallow	Land left unseeded during a growing season.
Shrublands	Natural vegetation lands with woody vegetation less than 2 m tall and with shrub canopy cover more then 10%. The shrub can be either evergreen or deciduous.
Badlands	Bare areas with exposed soil, sand, rocks, or erosion land, sparsely covered except for juniper, rose, and a selection of species from the goosefoot family during any time of the year.
Water bodies	Natural and artificial lakes, reservoirs, and rivers. Can be either fresh or salty water bodies.

2.4 Software used in this study

PCI Geomatics 9.1, ArcGIS 9.0, and SPSS 11.0 were applied on the data processing and analysis in this study. PCI was used to conduct image processing, ArcGIS was used to link raster data with vector data, and SPSS was used for statistical analysis.

Chapter 3 Topographic corrections on SPOT image for land cover classification

3.1 Introduction

One of the most common uses of satellite images is mapping land cover via image classification. However, classification of land-cover with remote sensing data has proven to be difficult in mountainous areas, and is quite often heavily influenced by shading caused by the terrain slope and aspect on recorded sensor signal response (Soenen, et al., 2005). Accuracy of electromagnetic levels measured remotely depends on many factors: spectral characteristic of the object, interaction of electromagnetic radiation in the atmosphere, sensor characteristic, and also on geometry: direction of sun illumination and sensor viewing direction (Hejmanowska, 1998). High relief can lead to topography related image distortions, while topographic slope and aspect can influence the natural spectral variability within any particular land-cover class. This effect is called “topographical effect”. It leads to high variation in the signal values (e.g., reflectance) between pixels with similar or even the same land cover types: shaded areas show less than expected reflectance, whereas in sunny areas the effect is the opposite, and further, causes the decrease of classification accuracy (Riano et al., 2003). Images of flat horizontal terrain with homogenous covering (forest, or soil, or grass) are different from images of the same covering but in a hilly area. This is caused by variation of the illumination direction, it means of zenith sun illumination angle (Dymond et al., 1999). A surface perpendicular to the sun at a low sun elevation will receive less radiation than a surface at a high solar elevation. Therefore, sun facing slope (southerly) seems to be brighter (warmer) than northerly facing slope. Due to atmospheric scattering, the solar elevation is also important (Hejmanowska, 1998).

Some studies show that topography can be one of the major sources of variation in remotely sensed data in high relief, mountainous areas (Goyal et al., 1999). It has been

found that 8-38% of the SAR image data variance to be caused by relief effects, whereas slope/aspect effects were responsible for 7–19% of the data variance of a test site in the Canadian Appalachian Mountains (Goyal et al., 1999). Franklin et al. (1995) found that topographic effects comprised 10–20% of the variability in SAR tone and texture measures in vegetated areas. In many cases, difference in reflectance coefficient measured remotely can be caused only by topographical effect. With the same physical characteristic for example the same forest type, different reflectance can be measured (Hejmanowska, 1998). In order to classify the satellite images effectively, removal of this "disturbing phenomena" or minimizing these effects is necessary before digital image classification. This process is called "topographic correction" or "topographic normalization", and it refers to the compensation of the different solar illuminations due to the irregular shape of the terrain (Riano et al., 2003). Topographic correction should reduce the internal variability of each land cover, and consequently, increase the classification accuracy. Therefore, the process of topographic normalization may be critical to achieve acceptable level of accuracy in areas of rough terrain as a preliminary step to the multispectral and multitemporal digital classification (Riano et al., 2003).

Topographic correction techniques have been widely applied in environment remote sensing, and can improve the accuracy of land cover classification (Colby, 1991; Ekstrand, 1996; Riano et al., 2003; Hejmanowska, 1998). Some correction methods, such as cosine, Minnaert, and C-correction, have been proposed and tested practically. Several authors have found that the non-Lambertian assumptions have performed well in the topographic normalization of vegetated surfaces. The most successful way to account for the vegetation being non-Lambertian has been to employ the Minnaert constant (Colby, 1991; Ekstrand, 1996), which has been used to describe the roughness of the surface. Colby (1991) developed a backward radiance correction model which utilizes the Minnaert constant based on the non-Lambertian assumptions. The method

can be used to minimize variation in values of brightness for similar surface materials caused by topographic conditions, shadows or seasonal changes in sun illumination factors. However, there is no clear consensus on methods that may be universally applicable. Some other researches showed that C-corrections retained best the spectral characteristics of each band and provided the highest reduction in class variability. Therefore, the main difficulty in applying topographic corrections is related to the lack of standard and generally accepted models.

Up to now, researches on topographic correction have only been conducted on satellite imagery in mountainous areas (Soenen et al., 2005). Some researchers believe that the effect of topography can be neglected if the slope is not too steep in the study area (Combal et al., 2002). There is no doubt that topography would increase the difference between the radiation scattered by topography and a flat surface at larger sun zenith angles. The objectives of this study are to assess the effectiveness of different topographic corrections for land cover classification on SPOT image in the gently rolling hills of the study area and compare the improvement of variability in several major land cover classes before and after topographic corrections. The performance of each procedure was assessed by two ways: 1) how they preserve the original spectral structure of the image, and 2) how they increase the statistical homogeneity of each land cover class, hence reducing the reflectance variations in interested classes caused by different illumination conditions. The influence of topographic correction on the classification accuracy was discussed in Chapter 4.

3.2 Current models for topographic correction on remote sensing image

The actual reflectance is dependent on the wavelength, and more severely, on the lighting, observation direction, and reflective properties of the surface. The reflectance properties are therefore best described by the so-called bidirectional reflectance

distribution function (BRDF). However, in any case all reflectance functions are class dependent. That means, if applied for performing radiometric corrections, the object classes have to be known in advance as they are input to the correction algorithm (Jansa, 1998). Therefore, topographic correction should be performed on each band and land cover class, respectively. The determination of BRDF is rather complex, since it describes the reflectance behavior at all possible angles of incidence, combined with all possible angles of reflection. As the BRDF is usually unknown or hardly determinable in practice, the directional reflectance is more feasible (Goyal et al., 1999).

At present, many topographic correction methods are based on modeling illumination (IL) conditions (Figure 3-1). These methods can be grouped into three categories: Lambertian, non-Lambertian, and statistical-empirical based methods. All the models require a suitable DEM based on which slope and aspect can be calculated, and also require detailed information on the date and time of day the image was acquired. Three representative methods in these categories are described as follows.

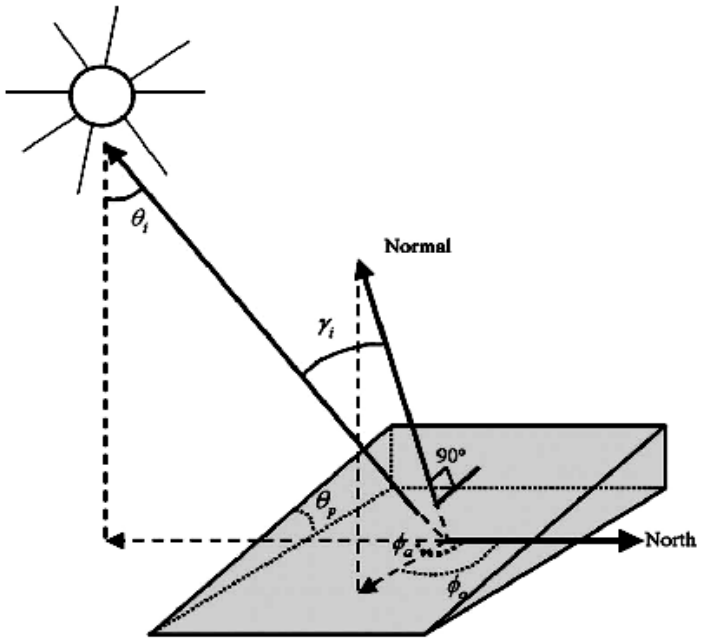

Figure 3-1 Angles involved in the computation of the IL (illumination): γ_i – the incident angle, θ_p – the slope angle, θ_i – the solar zenith angle, φ_α– the solar azimuth angle, and φ_o- the aspect angle.

3.2.1 Lambertian methods

In Lambertian method, the surface is assumed to have Lambertian behaviour, i.e. to be a perfect diffuse reflector, having the same amount of reflectance in all view directions, and the total irradiance received at a pixel is directly proportional to the cosine of the incidence angle. Thus, the Lambertian correction function attempts to correct only for differences in illumination caused by the orientation of the surface (Sandmeier et al., 1997). The cosine correction is the most wildly applied method for Lambertian correction.

The incident angle (γ_i) is defined as the angle between the normal to the ground and the sun rays, as shown in Figure 3-1.

Equation 3-1 shows the calculation of illumination conditions (IL).

$$IL = \cos \gamma_i = \cos \theta_p \cos \theta_z + \sin \theta_p \sin \theta_z \cos(\varphi_\alpha - \varphi_0) \quad (3\text{-}1)$$

where θ_p is the slope angle; θ_z is the solar zenith angle; φ_α is the solar azimuth angle; and φ_o is the aspect angle.

Based on IL from equation 3-1, cosine or Lambertian correction is implemented as:

$$\rho H = \rho T (\frac{\cos \theta_z}{IL}) \quad (3\text{-}2)$$

where ρH=slope-aspect corrected reflectance value, ρT=uncorrected reflectance value.

However, this approach is based on the following assumptions: reflectance from all surfaces is Lambertian, earth-sun distance is constant, and amount of solar radiation reaching the earth is constant, which is not applicable to most natural surfaces. Numerous tests of this approach have established that it does overcorrect shadowed areas, i.e., making them appear too bright (Riano et al., 2003).

3.2.2 Non- Lambertian methods

To address the "over-correction" resulting from the cosine Lambertian correction, the non- Lambertian method--Minnaert constant has been used in topographic corrections to represent the extent to which a surface is non-Lambertian (Soenen et al., 2005). The Minnaert constant correction is implemented as:

$$\rho H = \rho T (\frac{\cos \theta_z}{IL})^{K_k} \quad (3\text{-}3)$$

where K_k is the Minnaert constant for band k.

The Minnaert constant is used to describe the roughness of the surface. As a result, the problem of overcorrection in the area facing away from the sun may be solved.

It is necessary to calculate the value of *K* for each band before performing the correction, The Minnaert constant is empirically derived by: (1) logarithmically linearizing equation (3-3),

$$Log\ (\rho T) = Log\ (\rho H) + K * Log\ (\frac{IL}{\cos\ \theta_z}) \quad (3\text{-}4)$$

Y= a + k X

$Y = \text{Log}\ (\rho T)$

$$X\ = Log\ (\frac{IL}{\cos\ \theta_z})$$

a = log ρH

(2) obtaining a sufficiently large sampling size of pixels located on moderate to steep, east and west facing slopes (ρT- Values), and (3) estimating the value of the Minnaert constant using regular linear regression analysis (Riano, 2003).

This equation 3-3 was further modified to include the slope of the terrain to perform the topographic correction (Riano, 2003).

$$\rho H\ = \rho T\ \cos\ \theta_p\ (\frac{\cos\ \theta_z}{\text{IL}\ \cos\ \theta_p})^{\text{K}_\text{k}} \quad (3\text{-}5)$$

3.2.3 Statistical-empirical based methods

Another method is the empirical–statistical method with the assumption of a linear correlation between the reflectance and IL for each band.

$$\rho T\ = \rho H\ + m_k \text{IL} \quad (3\text{-}6)$$

Previous studies have demonstrated that some correlation exists between the predicted illumination derived from a digital elevation model and the measured illumination of a

target. Based on this correlation, a C-correction approach was developed that can be used with a linear regression to correct or normalize observed data (Civco, 1989). A regression between the cosine of the effective angle of incidence and the measured radiance generally show a positive linear correlation. The C-correction is defined as:

$$\rho H = \rho T \left(\frac{\cos \theta_z + c_k}{\mathrm{IL} + c_k}\right) \tag{3-7}$$

where c_k=b_k/m_k, for ρT= b_k + m_k IL, k=band.

And m_k and b_k were estimated using the regular linear regression analysis with the same procedures as that of calculating Minnaert constant.

The C value exerts a moderating influence on the cosine correction by increasing the denominator and reducing the over-correction of faintly illuminated pixels. The C-correction has been shown to retain the spectral characteristics of the data and improve overall classification accuracy in areas of rugged terrain. It can also be derived easily (Riano et al., 2003). Previous studies show that C-correction is the most effective illumination correction for Landsat data (Soenen et al., 2005).

3.3 Methods

3.3.1 Topographic correction evaluation

This study is based on a cloud-free SPOT image (June 22, 2005) that covers the west block of GNP and surrounding pastures. Information on the study area and image preprocessing has been described in Chapter 2. After geometric and radiometric/ atmospheric corrections, the SPOT reflectance data were further processed to reduce the radiometric distortion caused by topographic effects. The methods of Minnaert's model and C-correction were used to conduct the correction based on the previous studies.

Minnaert's model and C-correction have been widely used in the radiometric correction of topographic effects, and believed effective in reducing the topographic effects on the reflectance in mountainous areas (Tokola et al., 2001).

The value of *K* constants (Minnaert's model) and C coefficients (for C-correction) were calculated for each band of the entire image before performing the correction. The procedures for calculating *K* constants and C coefficients were described in section 3.2.

After calculating the Minnaert constants and C coefficients, topographic correction for each pixel of the entire image was performed using the equations 3-3 and 3-7, respectively, along with the data of the slope, aspect (from DTM), the solar azimuth, and solar zenith angles, which were shown in the image header file.

3.3.2 Field data and validation of topographic correction

Validation was performed by two methods: 1) comparing the mean and standard deviation (SD) between topographically corrected reflectance and the original reflectance calculated by radiometric and atmospheric correction for the whole image, and 2) comparing the change of reflectance mean and SD in each land cover class before and after the topographic correction. Change in the reflectance mean after correction should be low; otherwise it would imply an under- or over-correction. While the SD for each land cover class should be reduced, meaning a greater intra-class homogeneity has been achieved, and consequently, improve the classification of land cover. Also, responses of different slope (>1°, 1-5°, 5-25°, and >25°) and aspect class (southerly faced and northerly faced) to the topographic correction were examined.

For the purpose of this study, a total of 560 point based field samples with randomly stratified sampling design were collected in the summer of 2005. GPS readings (UTM

coordinates, elevation), land cover class, topography, plant cover percentage, and dominant species were collected for each point.

Six land cover classes, including grasslands, croplands, fallow, shrublands, badlands, and water bodies, were chosen to assess the changes in reflectance mean and SD. The field data were used to locate the land cover classes on the image and extract the pixel for analysis.

3.3.3 Outline of research method

Figure 3-2 summarizes the methods and procedures applied to perform topographic correction on SPOT image in this study.

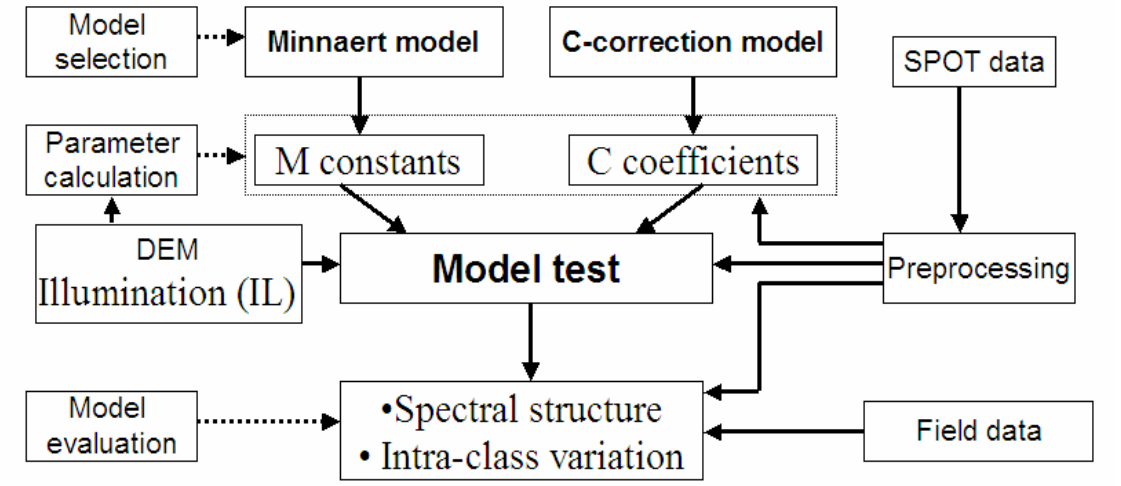

Figure 3-2 Flow chart of topographic correction.

3.4 Results and discussions

3.4.1 Minnaert constants and C coefficients

Table 3-1 shows the values of the Minnaert constant and C coefficient for each band as well as their respective goodness of fit as obtained from the statistics of the regression analysis performed on the SPOT image. It is interesting to note that the largest C coefficient and the smallest K constant were observed in the NIR band, an indication that near infrared band is more severely affected by the topographic effect.

Table 3-1 Minnaert constants and C coefficients for SPOT image*.

Band	C-correction			M-constant correction		
	C coefficient	R^2	Sig.	K constant	R^2	Sig.
Green	0.26719	0.14	0.046**	0.78155	0.22	0.005**
Red	1.01122	0.15	0.023**	0.61416	0.21	0.049**
NIR	1.46431	0.18	0.034**	0.39743	0.23	0.034**
MIR	0.21062	0.35	0.000**	0.96917	0.43	0.000**

* Sample size=93; ** significant at P<0.05 level.

3.4.2 Comparison of reflectance mean for the whole image

From the Figure 3-3 and Table 3-2 it can be found that the reflectance mean and standard deviation for each band after corrections are almost the same comparing to the original reflectance. It means that the two topographic corrections highly preserved the original spectral structure after topographic corrections on each SPOT band for the entire image and the image was not under- or over-corrected.

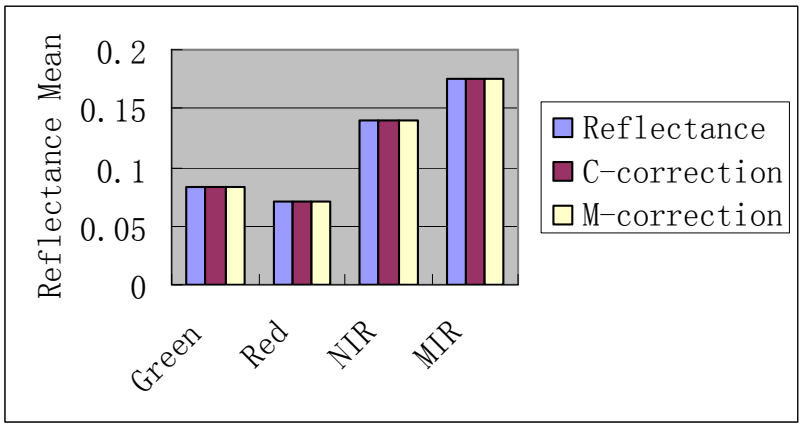

Figure 3-3 Reflectance means for each band before and after corrections.

Table 3-2 Reflectance statistics for the whole image.

		Green	Red	NIR	MIR
Original	Mean	0.0837	0.0704	0.1393	0.1755
reflectance	SD*	0.0558	0.0473	0.0888	0.1116
C-correction	Mean	0.0838	0.0705	0.1394	0.1759
reflectance	SD	0.0563	0.0473	0.0889	0.1199
M-correction	Mean	0.0838	0.0704	0.1392	0.1759
reflectance	SD	0.0559	0.0473	0.0887	0.1119

* SD-standard deviation.

3.4.3 Spectral change amongst land cover classes

Reflectance mean and standard deviations (SD) before and after the corrections for each land cover class were calculated and compared (Tables 3-3 and 3-4). Table 3-3 shows the original reflectance means of different cover classes were highly maintained for all land cover classes in each band after the two corrections, even though a slight decrease

among the two classes of shrublands and badlands.

Table 3-3 Comparison of reflectance means before and after topographic corrections for different land cover classes*.

	Land cover	Green	Red	NIR	MIR
Atmospheric corrected reflectance	Grassland	0.1052	0.0943	0.1882	0.2400
	Cropland	0.1728	0.0863	0.1868	0.2207
	Fallow	0.1240	0.1622	0.2629	0.3150
	Shrub	0.1538	0.0641	0.1573	0.1897
	Badland	0.1222	0.1637	0.2813	0.2835
	Water bodies	0.0264	0.0505	0.1325	0.0478
Minnaert corrected reflectance	Grassland	+0.09%	+0.06%	-0.02%	+0.20%
	Cropland	N	+0.02%	N	+0.05%
	Fallow	-0.14%	-0.14%	-0.10%	-0.19%
	Shrub	-0.85%	-0.89%	-0.80%	-0.95%
	Badland	-0.61%	-0.71%	-0.53%	-0.68%
	Water bodies	-0.08%	-0.06%	-0.05%	-0.08%
C-coefficient corrected reflectance	Grassland	+0.14	+0.20%	+0.12%	+0.22%
	Cropland	+0.03%	+0.05%	+0.03%	N
	Fallow	-0.08%	-0.18%	-0.10%	-0.18%
	Shrub	-0.48%	-0.75%	-0.46%	-0.81%
	Badland	-0.40%	-0.58%	-0.36%	-0.61%
	Water bodies	-0.04%	-0.08%	-0.06%	-0.08%

* -: mean decreases, +: mean increase, and N: no change in mean.

Table 3-4 Comparison of reflectance SDs before and after topographic corrections for different land cover classes*.

	Land cover	Green	Red	NIR	MIR
Atmospheric corrected reflectance	Grassland	0.0119	0.0114	0.0150	0.0185
	Cropland	0.0228	0.0214	0.0251	0.0335
	Fallow	0.0091	0.0131	0.0153	0.0233
	Shrub	0.0195	0.0079	0.0098	0.0214
	Badland	0.0136	0.0204	0.0292	0.0420
	Water bodies	0.01038	0.0063	0.0156	0.0113
Minnaert corrected reflectance	Grassland	+0.67%	-0.60%	+0.27%	-0.76%
	Cropland	+0.09%	-0.20%	-0.32%	0.27%
	Fallow	-0.44%	-1.30%	-1.20%	-1.50%
	Shrub	-1.40%	-5.70%	-8.50%	-13.40%
	Badland	3.20%	-2.70%	-3.20%	+2.90%
	Water bodies	+0.09%	-0.47%	-0.26%	N
C-coefficient corrected reflectance	Grassland	+0.50%	-0.72%	+0.2%	-0.92%
	Cropland	+0.09	-0.31%	-0.36%	-0.27%
	Fallow	-0.33%	-1.70%	-1.25%	-1.50%
	Shrub	-1.30%	-5.45%	-7.03%	-5.29%
	Badland	-1.90%	-0.15%	-1.20%	+2.48%
	Water bodies	+0.02%	-0.50%	-0.20%	+0.17%

* -: SD decreases, +: SD increases, and N: no change in SD; SD: standard deviation

If the topographic correction is successful, the standard deviation of each class should decrease. In terms of standard deviation (SD), the Minnaert constant and C-correction show decreases among most of the land cover classes, though the decrease was not

dramatic (Table 3-4). The larger decrease of SD was observed in shrubland and badland. Two infrared bands, NIR and MIR, reached greater decreases in SD among the four bands. Figure 3-4 shows that the SDs reduced in NIR band for all land cover classes after topographic corrections. However, there are no dramatic differences between the Minnaert constant and C-correction in decreasing the SD. A decrease in SD implies greater intraclass homogeneity. No doubt, the decrease of SD in the SPOT image should benefit the classification to some extent. Also, green band shows an increase in the SD for most of the classes after the two corrections. This may be explained by the fact that shorter wavelengths are easily affected by the scattering effect.

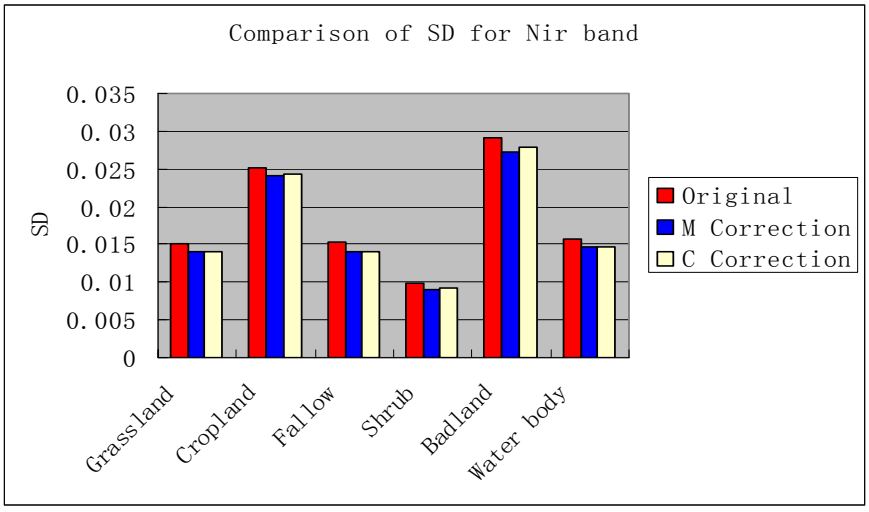

Figure 3-4 Standard deviation (SD) change among land cover classes in NIR band.

3.4.4 Spectral change with slopes and aspects

Table 3-5 and 3-6 show the reflectance means and standard deviations change for different slopes and aspects. Reflectance means on the sunny slopes are expected to decrease while those on the shady side are expected to increase for a successful topographic correction. Table 3-5 shows that there is a significant increase in reflectance

mean on northerly-faced slope and a decrease on southerly-faced slope in each band for the two corrections comparing to the original reflectance mean, whereas the reflectance mean for horizontal terrain is similar to the original reflectance. Reflectance mean changed more with the slope angle increasing. When the slope is greater than 25 degrees, over-correction was observed on northerly faced aspect. The two corrections have similar effects in this point. This supports and confirms the general observation of overcorrection for steep slope on shady areas in the previous researches (Thomson et al., 1990; Jones et al., 1988).

There are slight decreases in the standard deviations on the sunny slope for most bands after the two corrections. However, the Minnaert correction and C-correction all show an increase in the standard deviations on shady side in all bands, especially when the slope is greater than 25 degrees. This may be caused by the overcorrection in the shadow areas with steep slopes.

The errors of topographic correction increase with the slope and incidence angle. In general, the correction is very unreliable and inaccurate for shady slopes with incidence angles greater 90° along the mountain range or for areas having sudden changes from dark to bright. Pixels that had incidence angle over 80 degrees were overcorrected. In addition, for the estimate of Minnaert constant and C-coefficient, choosing different samples usually produces different constant and coefficient estimates, therefore, results in different terrain-corrected images. Samples selected in all areas across the entire scene will work reasonably well for the topographic correction.

Table 3-5 Comparison of reflectance means before and after topographic corrections for different slopes and aspects*.

	Aspect	Southerly faced			Northerly faced			Horizontal
	Slope	1-5º	5-25º	>25º	1-5º	5-25º	>25º	<1º
R	Green	0.1274	0.1223	0.1034	0.1014	0.1115	0.0990	0.1198
	Red	0.1083	0.0851	0.1033	0.0952	0.0919	0.0934	0.1087
	NIR	0.2092	0.1808	0.2012	0.1908	0.1877	0.1892	0.2044
	MIR	0.2503	0.2288	0.2429	0.2359	0.2093	0.2367	0.2585
M	Green	-0.81%	-4.20%	-12.56%	+1.22%	+7.08%	+34.88%	N
	Red	-0.81%	-4.00%	-13.23%	+1.19%	+6.23%	+34.32%	N
	NIR	-0.56%	-3.23%	-16.31%	+0.75%	+3.33%	+11.85%	+0.005%
	MIR	-1.18%	-5.21%	-8.06%	+1.84%	+11.3%	+75.78%	N
C	Green	-0.66%	-2.99%	-2.60%	+1.05%	+6.56%	+30.29%	+0.008%
	Red	-1.02%	-4.33%	-3.63%	+1.60%	+9.45%	+58.53%	N
	NIR	-0.62%	-2.67%	-2.29%	+0.95%	+5.54%	+27.52%	+0.01%
	MIR	-1.11%	-4.72%	-4.03%	+1.74%	+10.8%	+65.98%	N

* R: original reflectance, M: Minnaert constant-corrected reflectance, and C: C-coefficient-corrected reflectance; -: mean decreases, +: mean increases, and N: no change in mean.

Table 3-6 Comparison of reflectance SDs before and after topographic corrections for different slopes and aspects*.

	Aspect	Southerly faced			Northerly faced			Horizontal
	Slope	1-5º	5-25º	>25º	1-5º	5-25º	>25º	<1º
R	Green	0.0313	0.0249	0.01249	0.01631	0.01961	0.01173	0.02226
	Red	0.0309	0.0119	0.01456	0.01407	0.02703	0.00992	0.02422
	NIR	0.0378	0.0144	0.01907	0.02003	0.03467	0.0129	0.03318
	MIR	0.0365	0.0190	0.01602	0.01797	0.03256	0.01155	0.03342
M	Green	-0.38%	-6.26%	+4.00%	+0.92%	+16.2%	+25.75%	-0.09%
	Red	-0.87%	-0.75%	-20.94%	+1.14%	+3.77%	+127.6%	0.04%
	NIR	-0.53%	+2.78%	-14.74%	+0.60%	+1.01%	+41.08%	-0.03%
	MIR	-1.17%	-2.99%	-1.69%	+3.22%	+14.6%	754.98%	+0.18%
C	Green	-0.32%	-4.13%	-4.16%	+0.80%	+15.2%	-2.22%	-0.09%
	Red	-1.10%	-1.84%	+6.87%	+1.56%	+5.99%	+224.6%	+0.04%
	NIR	-0.61%	+0.07%	+6.87%	+0.80%	+1.70%	+16.36%	N
	MIR	-1.12%	-3.15%	+22.0%	+3.01%	+13.7%	+529.9%	+0.15%

* SD: standard deviation, R: atmospheric-corrected reflectance, M: Minnaert Constant-corrected reflectance, and C: C-coefficient-corrected reflectance; -: SD decreases, +: SD increases, and N: no change in SD.

3.5 Conclusions

The results from the topographic correction evaluation of this study demonstrated that some of the radiometric variation caused by terrain slope and aspect can be reduced using non-lambertian surface assumption based methods (Minnaert model) and semiempirical model (C correction). Furthermore, reducing variations among land cover classes will benefit the classification accuracy to some extent.

From the results of this study, the following conclusions may be derived:

(1) Both of the correction models applied in this study can be effective at reducing radiometric variation among land cover classes caused by topographic effect in the study area featured by the gently rolling hills and mixed-grassland prairie. This achieves better intraclass homogeneity in land cover classes. However, the two topographic corrections applied in this study did not obtain significant reduction in variations for the interested land cover classes. Part of the reason may be the less solar zenith of the sensor and relatively flat study area. Although the improvement of variation is minor in the relatively flat areas of this study, the topographic correction should logically improve the classification accuracy to some extent.

(2) The two topographic correction methods provide a simple and effective way to reduce the variation in data caused by the topographic effect. However, they seem unstable over a wide range of slope-aspect combinations or angles of incidence, and less effective for steeper terrain.

(3) Variance statistics based on image datasets are limited to a subset that can only test a limited number of terrain orientations. Even for the terrain being considered, it is difficult or impossible to know what constitutes a "correct" value on a pixel-by-pixel basis where the topographic effect is removed, and it is also difficult to locate reference validation pixels on flat terrain. A proper validation should consider a complete set of different slopes, aspects, and other vegetation attributes. However, more comparisons with the in situ measurements are needed to estimate the accuracy of the method.

(4) Minnaert constants and C correction coefficients are critical in the topographic correction applied in this study. The size of sample must be large enough and selected in all area across the entire image. However, the estimation of Minnaert constant and C

coefficient is a difficult task (Tokola et al., 2001).

(5) Eventually, it needs to emphasize that a high quality rectification together with an accurate DTM are crucial preconditions for a successful topographic normalization, independent of whether the normalization just serves as a preprocessing step or it is the final correction based on a more sophisticated mathematical and/or physical model.

Chapter 4 Comparison of maximum likelihood classification method with artificial neural network algorithm for land cover mapping

4.1 Introduction

Land cover refers to the suite of natural and man-made features that cover the earth's surface (Wessels et al., 2004). Concern over the state of the earth's environment has resulted in an increased need for accurate land cover information, which is applied in policy development, natural resource management, monitoring environmental change, carbon cycle studies, and modeling of biogeochemistry, hydrology, and climate (Latifovic et al., 2004; Boles et al., 2004). For different aspects of regional planning the authorities have to rely on up-to-date information about land cover of the planning area. Land cover changes through time due to human activities and natural disturbance. Under this dynamic situation, accurate, meaningful, and up-to-date data on land cover is essential and critical if public agencies and private organizations want to know what is happening, and to make sound plans for their own future action (Kerr et al., 2003). In rangeland insurance, the information of land cover is used to verify the pasture types and acreage the ranchers applied for participating in a rangeland insurance program in order to combat insurance fraud and abuse, assist in evaluating the regions impacted by climate change, and provide the background for local adjustment of insurance (Goodwin et al., 2004). The information of land cover is also used as the basis of yield calculation. Existing land cover data usually can not meet the requirements in implementing a rangeland insurance program (LaFrance et al., 2002).

Field based methods to map land cover over large area is difficult, if not impossible. Remote sensing has become a valuable tool for gathering land cover information at regional, continent, and globe level with a range of satellite data and spatial/spectral resolutions (Giri et al., 2005). The strength of satellite remote sensing for land cover

mapping is in the low cost per unit of land area associated with data capture and image analysis, the large area coverage, and the ability to easily acquire data over geographically isolated areas (Cihlar, 1998). Historically, land cover mapping has used either multitemporal or multispectral imagery depending on whether the study had global or continental extent with coarse resolution (typically using AVHRR datasets), or covered smaller areas with higher resolution (typically using Landsat and SPOT images (Lobo et al., 2004). Multitemporal imagery has the potential to map land cover because of the phenological differences between vegetative species. However, combining images of multiple dates presents special problems: difficulties in co-registering and obtaining cloud-free imagery during optimal periods (Hill et al., 1999). In addition, phenology is influenced by factors such as photoperiod, soil moisture, soil temperature, air temperature, and solar illumination. It is not always reliable to use phenological information in the classification, therefore, single-date image becomes an alternative in some situations (Sakamoto et al., 2005).

Image classification is a key component of remote sensing (Biscoff et al., 1992; Carmel et al., 1998). Up to now, a lot of algorithms have been developed to classify remote sensing data, from the traditional maximum likelihood classifier (MLC) to newly developed advanced artificial neural networks (ANNs). In theory, the MLC is considered to be the best classifier in the sense of obtaining an optimal classification rate (Qiu et al., 2004). In practice, however, because some assumptions have to be made about the probability distribution of features, such an optimum rate might be poorly approximated (Erbek et al., 2004). This is one of the major reasons why ANNs are increasingly applied to the classification of satellite images. ANNs are computational systems whose architecture and operation come from our present knowledge of biological nervous systems (Atzberger, 2004). Analogous to these systems, ANNs consist of a set of suitably positioned simple processing elements (nodes or neurons). An

ANN can realize any arbitrarily complicated, generically nonlinear functional relationship between its inputs and its outputs by superposition of the elementary node functions (Mutanga et al., 2004). The advantage of neural network methods is that no prior statistical information is needed about the input data, and it makes no assumptions about the nature of the data distribution (Kulkarni, 1998). The effectiveness of artificial neural networks to solve highly non-linear problems such as land-cover classification based on multispectral imagery has been demonstrated (Vieira, et al., 2000). However, there remains the question of how many neurons and layers are enough. Too few layers or neurons lead to underfitting, and too many neurons can contribute to overfitting. Overtraining occurs when the neural network "memorizes" specifics of the training data but is not able to generalize when applied to a different data set (Mutanga et al., 2004). When using back propagation (BP) algorithm, ANN may not come to convergence as the number of classified classes increases. Also, the increase in the number of nodes in each hidden layer does not have a significant effect on the overall accuracy (Erbek et al., 2004). Therefore, it remains to be evaluated in practical applications using operational satellite data and many land cover classes in representative environments.

A number of vegetation indices have been developed and used for monitoring land cover classification. The normalized difference vegetation index (NDVI), which uses spectral information from the red and near infrared bands, is most widely used. NDVI has served as the input data for various satellite-based land cover mapping activities (Defries et al., 1995; Loveland et al., 1997). Recently, normalized difference moisture index (NDMI), calculated using NIR and MIR, has been used together with NDVI as input to land cover mapping efforts, with the expectation that the increased amount of spectral information provided from NDMI would improve the discrimination of vegetation types (Cihlar et al., 1998). It is known that NDVI has several limitations including: sensitivity to both atmospheric conditions (Cihlar et al., 1998) and the soil

background, and a tendency to saturate at closed vegetation canopies with large leaf area index values. In addition, VIs based on the soil background adjustment, such as modified soil adjusted vegetation index (MSAVI) and adjusted transformed soil-adjusted vegetation index (ATSAVI), were also applied in vegetation and land cover classification (Qi et al., 1994). However, vegetation indices used in classification vary from one ecosystem to another in the literatures (Lawrence, et al., 2006). There is a requirement to assess the potential of other VIs for generating improved land cover classifications that take advantage of a much greater portion of the electromagnetic spectrum.

Image classification relies on the spectral distinctness and variability of classes. Topographic effect leads to a high variation in the reflectance response for similar vegetation types and causes a decrease in accuracy of the land cover classification (David Riaño, et al., 2003). The objective of this research was to compare the performance of two classification techniques--maximum likelihood classifier (MLC) and artificial neural network (ANN) under two topographic correction procedures, in terms of classification accuracy, for land cover classification in mixed prairie of this study area. Original reflectance and topographic corrected reflectance, along with their derived vegetation indices, were used as inputs into the classifiers for the purpose of comparison.

4.2 Methods

4.2.1 Field data

Field data collection was performed in later June and early July, 2005. A total of 560 point-based field samples were obtained and each field sample was located using a GPS (Garmine 76). The sample points were randomly selected from each land cover class.

Cover percentage, dominant species, and topographic data were collected at each point. At each point, only one land cover type was included at the extent of 60 m from the point location. Field data were used as training sites and for the assessment of classification accuracy.

4.2.2 Topographic correction

Two topographic correction models, Minnaert's model and C-correction model, were performed on the SPOT image. Detailed methods and results were described in Chapter 3.

4.2.3 Vegetation indices used in this study

More than 20 vegetation indices have been proposed and used at present (Tian et al., 1998). Among which, NDVI, modified soil adjusted vegetation index (MSAVI) are commonly used. They were proposed according to different research characteristics and the different research objects of the researchers. One research has indicated that there is good agreement between green plants' degree of cover and the biomass (Jensen, 2000). Generally speaking, NDVI and MSAVI are sensitive to the growth condition and the spatial distribution of green plant density and they are influenced strongly by the soil properties (Jensen, 2000).

Four VIs were tested in this study: normalized difference vegetation index (NDVI), one of the most common indices used in remote sensing studies and sensitive to low levels of vegetative cover; normalized difference moisture index (NDMI), which is sensitive to the water content of vegetation and soil; and MSAVI and adjusted transformed soil-adjusted vegetation index (ATSAVI), which account for the influence of the soil background. Lawrence et al. (1998) found that under conditions of high substrate and

vegetation heterogeneity, NDVI was highly correlated to green vegetation cover. In this study area, since the vegetation is characterized by lower leaf area index (LAI), influence to the reflectance from soil background can be significant. Therefore, ATSAVI and MSAVI may be useful in the land cover classification in this study area. Some researches showed that NDMI could improve the discrimination of vegetation types (Cihlar et al., 1998; Boles, et al., 2004). Thus, NDMI was selected as a variable in land cover classification.

ATSAVI (Baret et al., 1991) can minimize the soil background influence by establishing a soil line to characterize the soil spectra (Qi et al., 1994). The actual gain (a) and intercept (b) values of the soil line and an adjustment factor (X) were considered for ATSVAI to minimize the soil background effects ($X = 0.08$ in the original paper by Baret and Guyot, 1991).

The four VIs were calculated using original reflectance and topographic corrected reflectance, respectively. The formulas for calculating the four VIs were listed in Table 4-1.

Table 4-1 Vegetation indices used in land cover classification.

VIs	Formula	Reference
NDVI	$\frac{NIR - Red}{NIR + Red}$	Haboudane et al., 2004
NDMI	$\frac{NIR - MIR}{NIR + MIR}$	Labrecque et al., (2006)
MSAVI*	$\frac{NIR - Red}{NIR + Red + L} * (1 + L)$	Tian et al., 1998
ATSAVI*	$\frac{a(NIR - aRed - b)}{aNIR + aRed - ab + X(1 + a^2)}$	Baret and Guyot, 1991

* X=0.08, α is 1.22, b is 0.03, and L=0.5 in the study area.

4.2.4 Band and VI selection as inputs to the classifiers

Common problems in the area of remote sensing classification involving data relevancy include selecting optimal number of bands and finding appropriate classification methods (Benediktsson, et al*.,* 1997). One would expect that as the number of bands increases, the accuracy of classification should also increase. This is not always true. Redundancy in data can cause convergence instability of models, and variations due to noise in redundant data propagate through a classification or discrimination model. Thus, processing a large number of bands with redundancy can result in higher classification inaccuracy than processing a subset of relevant bands without redundancy. On the other hand, fewer bands do not guarantee the best discrimination between data classes, because they do not accommodate distinct signal sources for all the classes (Chang et al., 2006).

It is very difficult and challenging to determine how many bands are needed in order to preserve necessary information. Existing band selection strategies (Warner et al., 1997) are not designed to select specified numbers of bands from predetermined groupings of

bands. For example, it would require a complex algorithm to identify proper bands from all the possible combinations (Key et al., 2001). Chang et al. (2006) indicated that it requires at least the same number of bands as the classes to accommodate distinct signal sources. According to this idea, at least 6 bands should be included as inputs to the classifiers in this study.

The other problem is the criterion to be used for band selection. So far, there have been many methods developed to deal with this issue. However, some problems arise from using these approaches and no methods may be universally applicable. For simplicity, a simple spectral separability index (SSI, developed by Bruce et al., 2002) to assess the separability among classes in a given band/VI was used as criterion to select bands and VIs (equation 4-1). SSI takes into account both the inter-class and intra-class variabilities. A higher inter-class variability and smaller intra-class variability will result in a larger SSI value, the larger the SSI, the better the spectral separability.

$$SSI_{ij} = (Mean_i - Mean_j)^2 \times \left(\frac{1}{SD_i^2} + \frac{1}{SD_j^2}\right) \quad (4\text{-}1)$$

where, SSI_{ij} — spectral separability index between class i and j

Mean —average reflectance for class i and j

SD — standard deviation for class i and j.

The performance of bands and vegetation indices were evaluated with SSI on SPOT images in the study area, and bands or VIs with higher SSI were included in the band combination as inputs to the classifiers.

4.2.5 Supervised classification: maximum likelihood classifier

The supervised maximum likelihood classifier (MLC), which is the most common technique presented in the literature, was selected as the land cover classification

technique with which to compare with the ANN technique. MLC evaluates both variance and covariance of the training set data and uses these values to classify the image pixels. The classifier rules are based on an assumption that the frequency distribution of the class membership can be approximated by the multivariate normal distribution. Training data were used to determine the parameters of the probability function, variance-covariance matrix and mean, and applied to algorithms that compare the image pixels to the training set data and grouped the image pixels into the classes they most closely resemble. MLC requires sufficient representative spectral training sample data for each class to accurately estimate the mean vector and covariance matrix needed by the classification algorithm. If the training samples are not sufficient, the class mean vector and covariance matrix, which are the representatives of the classes, will be estimated inaccurately, and as a result, the classification accuracy will be lower (Erbek et al., 2004).

4.2.6 Supervised artificial neural network (ANN)

A back-propagation algorithm based ANN was applied to compare with the conventional MLC in the land cover classification. The term "back-propagation" refers to the training method by which the connection weights of the network are adjusted.

The back-propagation network is a type of multilayer feed-forward network. A neural network based on back-propagation algorithm consists of interconnected processing elements called units ("nodes" or "neurons"), which are organized in three or more layers. There is an input layer of units which are activated by the input image data (Erbek et al., 2004). The output layer of units represents the output classes to train for. In between, there are usually one or more hidden layers of units (which are either input units or output units). A unit in one layer is connected to all units in the next layer (Atzberger, 2004). A unit in a hidden or output layer receives input from all units in the

previous layer and produces one output value. Each link from a unit to the next layer's units has a weight, which suppresses or allows the output value from the unit (Figure 4-1). Once the network has been trained, it uses the input image data to activate the input layer, and then it goes forward through the network and uses the activation of the output layer units to produce the output imagery. The sigmoid function was used as an activation function to produce the unit's output. The second phase in training is a backward pass through the network to reduce the error between the actual and the desired output. This involves determining the errors and then calculating and adding weight adjustments to the neural network weights to lower the errors (PCI, 2003).

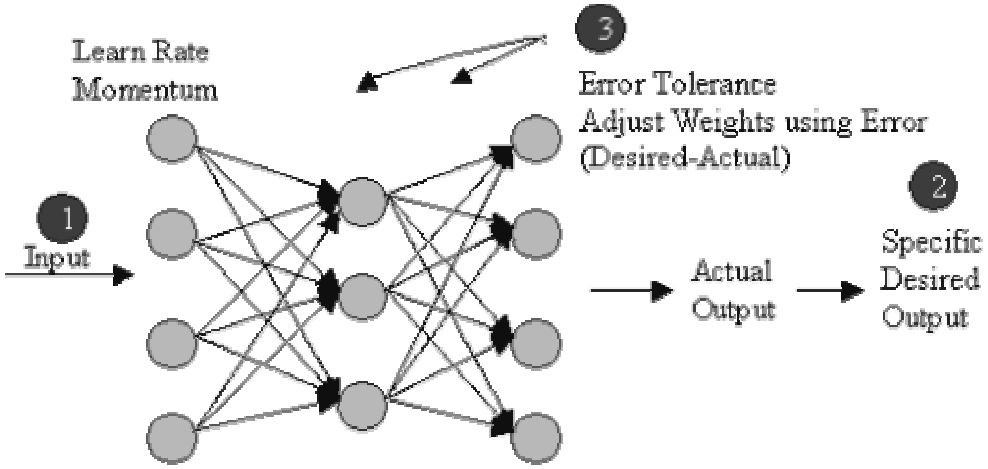

Figure 4-1 A typical structure design of ANNs.

Typically, back-propagation neural networks require a number of iterations before the interconnection weights stabilize enough to recognize the input patterns. The learning and momentum rates affect how quickly the neural network stabilizes. A high learning rate (0.9) would converge quickly, but may exit prematurely. A low learning rate (0.1) would take more iterations to train, but will not exit prematurely. The danger of a high learning rate is the modelling may oscillate and not stabilize. It can be observed that how different learning rates converge by examining the error plot in the output report.

The momentum rate can be used to speed up learning. A high momentum rate (0.9) trains with larger steps than a lower rate (0.1). Use of a momentum term helps reduce oscillation between iterations, and allows a higher learning rate to be specified without the risk of non-convergence (PCI, 2003).

Bishop (1995) indicated that any form of a decision region can be created by using a network with two hidden layers. Kanellopoulos et al. (1997) indicated that a single hidden layer network is appropriate for most remote sensing classification problems. A two-hidden-layer network should be used if the number of classes nears 20, allowing for the additional flexibility that such a complex problem requires (Kanellopoulos, et al., 1992). If a two hidden layer network is used, the first layer should have at least twice as many nodes as the number of inputs and perhaps even four times as many. The second hidden layer should have two to three times as many nodes as the number of output classes (Kanellopoulos et al., 1997).

In this study, a 4-layer network design, one input layer, two hidden layers (16 nodes for each layer) and one output layer, was used to perform the classifying.

4.2.7 Training data, test data and accuracy assessment

Both MLC and ANN need training sets to perform the algorithms. For the purpose of comparison, the same training sets and same samples for accuracy assessment were applied for the two classifiers, respectively. Training data from more than one sample point were required for each class because of the spectral variation and differences in illumination conditions within each class. A total of 121 field collected points were used as training sets, and each point was buffered by 20 meters to represent the four pixels of SPOT imagery. Other 439 points were used to assess the classification accuracy. So, sufficient training sets and assessment samples were ensured for each class.

An error matrix with three types of accuracies was generated for remote sensing classification accuracy assessment: overall accuracy, producer's accuracy, and user's accuracy. The overall accuracy of a classification can be found by dividing the total correct pixels by the total number of pixels in the error matrix. Producer's accuracy is the number of correctly classified pixels divided by the total number of reference pixels (column total), which shows the probability of a reference pixel being classified correctly. User's accuracy is the total number of correctly classified pixels divided by the total number of pixels classified as that class (row total), which defines the probability that a pixel classified represents that on the ground. Also, the kappa coefficient was calculated, which is a measure of the proportional (or percentage) improvement by the classifier over a purely random assignment to classes (Equation 4-2).

$$kappa = \frac{N\sum_{i=1}^{r} x_{ii} - \sum_{i=1}^{r} (x_{i+} * x_{+i})}{N^2 - \sum_{i=1}^{r} (x_{i+} * x_{+i})} \quad . \qquad (4\text{-}2)$$

where:

r = the number of rows in the error matrix

x_{ii} = the number of observation in row *i* and column *i*

x_{i+} = the marginal totals of row *i*

x_{+i} = the marginal totals of column *i*

N = the total number of observations.

Each of the six land cover classification combinations (labeled R-MLC, C-MLC, M-MLC, R-ANN, C-ANN, and M-ANN) was assessed for accuracy using contingency matrices. R stands for the original reflectance, M for reflectance from Minnaert Correction, and C for reflectance from C-correction.

4.2.8 Outline of research method

Figure 4-2 outlines the procedures for the comparison of classification algorithms in this study.

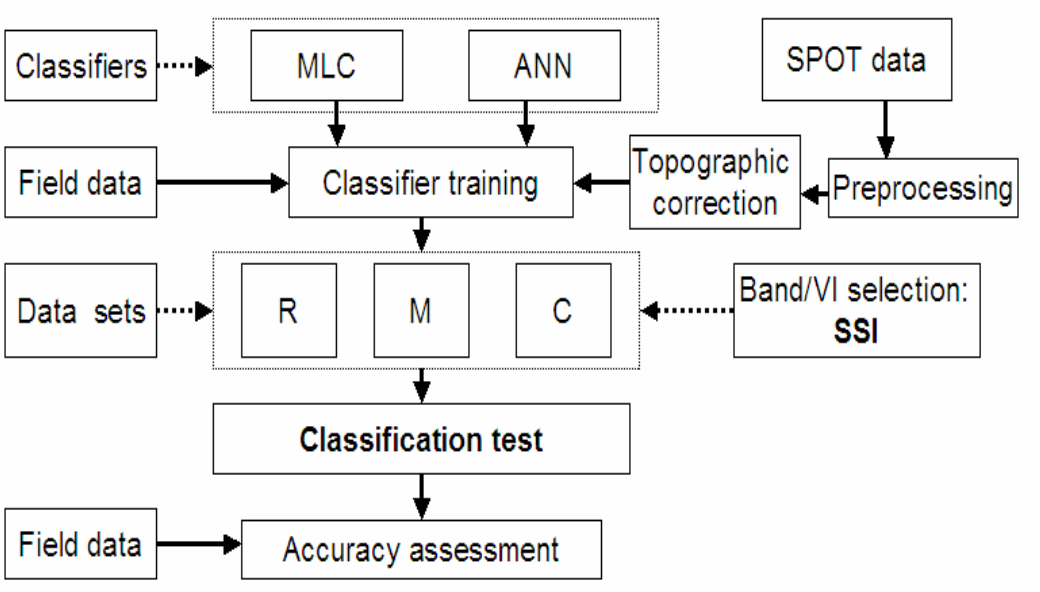

Figure 4-2 Flow chart for the comparison of classification algorithms. R represents the original reflectance + derived vegetation indices(VIs)M represents the reflectance from Minnaert correction + derived vegetation indices(VIs), and C represents the reflectance from C correction + derived vegetation indices(VIs). SSI=spectral separability index, MLC=maximum likelihood classifier, and ANN=artificial neural network.

4.3. Results and discussions

4.3.1 Spectral separability of the land cover classes and band/VI selection for classification

Whether or not land cover identification is possible using remote sensing data is determined by variation within land cover class and variation between spectra of different land cover classes. An efficient methodology for the discrimination of land cover hinges on significantly smaller spectral variation within the same class than that amongst different classes.

As shown Chapter 3, the topographic corrections can suppress the spectral variation within land cover class and thus can enhance the spectral separability of land cover classes. Table 4-2a, 4-2b, and 4-2c list the between-class separability (SSI) for the original reflectance, two topographic correction transformed reflectance, and corresponding VIs derived from the three data sets, respectively. The lowest separability values approaches 0 were observed between grasslands and croplands in the NIR band, cropland and fallow, cropland and shrubs in NDMI, and fallow and badlands in the red band in the three data sets. The large intra-class variation and large overlap of standard deviation for the classes at these bands or VIs explains their lowest separability. The best separability is between fallow and shrub in the red band for the three data sets. Overall, both the red band and NDVI reached better separability for most of the land cover classes, while the worse separability is consistently observed in NDMI and MSAVI for the three data sets. The trend in the three datasets is very similar, though each class displays a different separability in a specific band or VIs. It is worth noticing that the VIs derived from topographic correction transformed data sets obtained slight improvement in SSI. However, NDVI and ATSAVI showed a higher separability than SPOT bands such as Green and MIR band for most of the land cover classes. This

indicates that VI is useful in improving classification.

Table 4-2a Spectral separability (SSI) for original reflectance*.

	Green	Red	NIR	MIR	NDVI	NDMI	MSAVI	ATSAVI
Grass-Crop	**41.0**	0.7	*0.02*	1.4	5.5	2.8	9.3	9.7
Grass-Fallow	6.8	**62.4**	48.4	26.9	62.2	*2.3*	12.9	38.1
Grass-Shrub	22.8	21.7	14.1	13.0	**31.6**	*1.7*	9.6	24.7
Grass-Badland	3.6	**49.3**	48.8	6.6	37.1	24.6	*2.0*	6.2
Crop-Fallow	33.6	46.3	34.2	24.4	**84.3**	*0.1*	26.0	47.8
Crop-Shrub	1.7	8.9	**10.3**	2.9	3.5	*0.1*	6.0	0.9
Crop-Badland	18.8	28.3	25.5	5.8	**68.8**	9.3	*2.0*	25.9
Fallow-Shrub	13.1	**210.7**	163.6	63.3	182.7	*4.3*	33.2	90.1
Fallow-Badland	5.9	*0.02*	1.9	2.4	7.1	15.5	**17.3**	16.1
Shrub-Badland	8.0	**184.5**	178.9	24.2	161.5	11.7	*2.0*	52.1

* The highest and lowest separability values for each land cover class pair are **highlighted** (the highest) or in *italics*(the lowest). Water bodies were omitted.

Table 4-2b Spectral separability (SSI) for C corrected reflectance*.

	Green	Red	NIR	MIR	NDVI	NDMI	MSAVI	ATSAVI
Grass-Crop	**40.1**	0.7	*0.02*	1.5	5.6	2.8	9.1	9.6
Grass-Fallow	6.5	**62.9**	48.6	26.7	62.4	*2.5*	12.9	38.0
Grass-Shrub	21.3	23.7	16.4	14.9	**32.3**	*2.0*	9.0	24.1
Grass-Badland	3.0	**48.3**	47.7	6.0	36.4	25.2	*1.8*	6.2
Crop-Fallow	34.3	46.9	34.6	24.6	**84.8**	*0.1*	26.1	47.9
Crop-Shrub	1.9	9.9	**12.1**	3.5	3.7	*0.1*	0.1	0.9
Crop-Badland	18.5	27.4	24.7	5.4	**67.6**	9.5	*2.1*	26.0
Fallow-Shrub	12.5	**226.1**	182.5	69.1	185.2	*0.00*	32.8	89.4
Fallow-Badland	0.1	*0.01*	1.8	2.6	7.2	15.7	**17.1**	16.2
Shrub-Badland	7.5	196.4	**200.2**	26.0	160.6	11.4	*1.8*	51.6

* The highest and lowest separability values for each land cover class pair are **highlighted** (the highest) or in *italics* (the lowest). Water bodies were omitted.

Table 4-2c Spectral separability (SSI) for M corrected reflectance*.

	Green	Red	NIR	MIR	NDVI	NDMI	MSAVI	ATSAVI
Grass-Crop	**40.1**	0.7	*0.01*	1.5	5.8	2.9	9.6	10.0
Grass-Fallow	6.5	**63.1**	48.4	26.5	62.5	*2.6*	12.6	37.9
Grass-Shrub	21.2	24.7	17.4	15.1	**32.8**	*1.9*	8.6	24.0
Grass-Badland	3.0	**47.6**	46.9	5.8	36.2	25.5	*1.9*	6.1
Crop-Fallow	34.3	47.0	34.6	24.6	**85.4**	*0.1*	26.0	48.1
Crop-Shrub	1.9	10.4	**13.1**	3.6	3.7	*0.1*	0.2	0.8
Crop-Badland	18.4	26.8	24.1	5.3	**67.7**	9.5	*2.1*	26.8
Fallow-Shrub	12.3	**233.6**	191.2	69.7	186.3	*0.00*	30.9	87.3
Fallow-Badland	0.1	*0.00*	1.6	2.7	7.3	15.6	**16.9**	16.4
Shrub-Badland	7.4	201.6	**208.4**	26.1	160.8	11.7	*1.6*	51.3

* The highest and lowest separability values for each land cover class pair are **highlighted** (the highest) or in *italics*(the lowest). Water bodies were omitted.

Based on the spectral separability index, four SPOT bands and derived NDVI and ATSAVI were selected as combinations for the three data sets and as inputs to the classifiers (Table 4-3). The bands or VIs selected were the same for the three data sets based on their SSI. Using the same combinations made the comparison among different data sets and classifiers reasonable with the same baseline.

Table 4-3 Bands/VIs selected for the land cover classification.

Data sets	Selected bands/VIs
Reflectance	Green, Red, NIR, MIR, NDVI, ATSAVI
C-correction	Green, Red, NIR, MIR, NDVI, ATSAVI
M-correction	Green, Red, NIR, MIR, NDVI, ATSAVI

4.3.2 Classification accuracy of MLC

The overall accuracy, Kappa statistic, and producer's accuracy, and user's accuracy of

each class for the three data sets using MLC are listed in Tables 4-4, 4-5, and 4-6. In these tables, the numbers in each row represented the total ground sample points of a specific land cover class classified as different land covers. The classification accuracies for the three data sets–R, C, and M– were higher, and obtained the overall accuracy of 86%, 90%, and 89%, respectively. The individual class accuracy trends are similar for the three data sets. Individual class accuracies reveal that grassland is the most accurately identified land cover class followed by cropland and fallow (water body was excluded from the analysis because of its easy detection and less acreage in the study area). The least accurate class is shrub as many croplands were misclassified as shrub. This can be caused by the lower separability between shrub and cropland. Carefully examining the SSI for each class it can be found that the accuracy for individual class is consistent with its separability, and higher separability provided higher classification accuracy.

Table 4-4 Error matrix for MLC-R.

Class	Gras-land	Crop-land	Fallow	Shrub	Bad-land	Water bodies	Total	User's Accuracy (%)
Grassland	**233**	3	0	2	4	0	242	96.3
Cropland	4	**58**	2	1	0	0	65	89.2
Fallow	2	2	**27**	0	1	0	32	84.4
Shrub	19	10	0	**17**	0	0	46	37.0
Badland	2	1	2	0	**26**	1	32	81.3
Water bodies	0	0	0	0	0	**22**	22	100.0
Total	260	74	31	20	31	23	**439**	
Producer's accuracy (%)	89.6	78.4	87.1	85.0	83.9	95.7		
Overall accuracy = 86.4%						Kappa = 0.798		

Table 4-5 Error matrix for MLC-C.

Class	Grass-land	Crop-land	Fallow	Shrub	Bad-land	Water bodies	Total	User's Accuracy (%)
Grassland	**235**	2	1	1	3	0	242	97.1
Cropland	4	**59**	2	0	0	0	65	90.8
Fallow	3	1	**27**	0	1	0	32	84.4
Shrub	19	6	0	**21**	0	0	46	45.7
Badland	2	0	1	0	**28**	1	32	87.5
Water bodies	0	0	0	0	0	**22**	22	100.0
Total	263	68	31	22	32	23	**439**	
Producer's accuracy (%)	89.4	86.8	87.1	95.5	87.5	95.7		
Overall accuracy =89.1%						Kappa =0.827		

Table 4-6 Error matrix for MLC-M.

Class	Gras-land	Crop-land	Fallow	Shrub	Bad-land	Water bodies	Total	User's Accuracy (%)
Grassland	**236**	2	1	1	2	0	242	97.5
Cropland	5	**59**	1	0	0	0	65	90.8
Fallow	3	1	**26**	0	2	0	32	81.3
Shrub	20	6	0	**20**	0	0	46	43.5
Badland	1	0	1	0	**29**	1	32	90.6
Water bodies	0	0	0	0	0	**22**	22	100.0
Total	265	68	29	21	33	23	**439**	
Producer's accuracy (%)	89.1	86.8	89.7	95.2	87.9	95.7		
Overall accuracy = 90.5%						Kappa = 0.838		

The overall trends show that topographic correction can improve the land cover classification by 3-4% comparing to the original reflectance, and M-correction obtained a slightly higher (1%) accuracy than C-correction. This can be explained by the fact that topographic correction, whether M or C, can reduce the intra-class variation, and consequently, improve the classification to some extent. The improvement of land cover classification by employing the topographic corrections is slight; and the reasons for this result may lie in the less solar zenith of the sensor and relatively flat terrain in the study area. However, topographic correction is useful for classification, even in gently rolling areas like GNP.

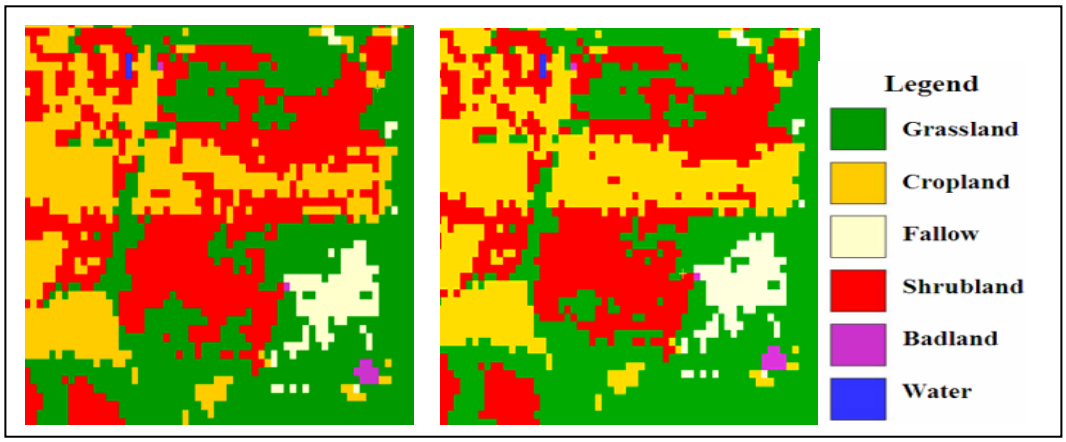

Figure 4-3 Comparison of classification maps (local) before (left) and after (right) the Minnaert model correction.

4.3.3 Classification accuracy of ANN

The overall accuracy, Kappa statistic, producer's accuracy and user's accuracy of each class for the three data sets using ANN were listed in Tables 4-7, 4-8, and 4-9 (the numbers in these tables have the same meanings as Tables 4-4, 4-5, and 4-6). The overall classification accuracies for the three data sets-R, C, and M- were 82%, 83%, and 85%, respectively, and slightly lower when comparing to the results generated from MLC. The individual class accuracy trends and overall trend of classification accuracy for the three data sets were very similar to the results generated from MLC. Individual class accuracies reveal that grassland is the most accurately identified land cover class, followed by cropland and fallow. For the same reason, water bodies were excluded from the analysis. The least accurate class is shrub. The overall trends show that topographic correction can improve the land cover classification by 3-4%, and M-correction obtained a 2% slightly higher accuracy than C-correction. This also can be explained by the fact that topographic correction, whether M or C, reduced the intra-class variation.

Table 4-7 Error matrix for ANN-R.

Class	Gras-land	Crop-land	Fallow	Shrub	Bad-land	Water bodies	Total	User's Accuracy (%)
Grassland	**214**	17	3	3	4	1	242	88.4
Cropland	4	**56**	1	0	4	0	65	86.2
Fallow	2	3	**26**	0	1	0	32	81.3
Shrub	23	5	1	**14**	0	3	46	30.4
Badland	2	0	1	0	**26**	3	32	81.3
Water bodies	0	0	0	0	0	**22**	22	100.0
Total	245	81	31	18	35	29	**439**	
Producer's accuracy (%)	87.4	69.1	83.9	77.8	74.3	75.9		
Overall accuracy =81.6%						Kappa =0.687		

Table 4-8 Error matrix for ANN-C.

Class	Gras-land	Crop-land	Fallow	Shrub	Bad-land	Water bodies	Total	User's Accuracy (%)
Grassland	**216**	16	3	3	3	1	242	89.2
Cropland	3	**56**	1	0	5	0	65	86.2
Fallow	2	3	**26**	0	1	0	32	81.2
Shrub	23	6	0	**14**	0	3	46	30.4
Badland	3	0	1	0	**26**	2	32	81.3
Water bodies	0	0	0	0	0	**22**	22	100.0
Total	247	81	31	17	35	28	**439**	
Producer's accuracy (%)	87.5	69.1	83.9	82.4	74.3	78.6		
Overall accuracy =82.9%						Kappa =0.718		

Table 4-9 Error matrix for ANN-M.

Class	Gras-land	Crop-land	Fallow	Shrub	Bad-land	Water bodies	Total	User's Accuracy (%)
Grassland	**224**	12	0	2	4	0	242	92.6
Cropland	1	**63**	0	0	1	0	65	96.9
Fallow	3	1	**25**	0	3	0	32	78.1
Shrub	23	7	0	**15**	1	0	46	32.6
Badland	0	0	1	0	**31**	0	32	95.9
Water bodies	0	0	0	0	0	**22**	22	100.0
Total	251	83	26	17	40	22	**439**	
Producer's accuracy (%)	89.2	75.9	96.2	88.2	77.5	100.0		
Overall accuracy =84.7%						Kappa =0.758		

4.3.4 Comparison of MLC and ANN

The MLC outperformed the ANN in the land cover classification in the study area using SPOT images, regardless of the fact that ANN has frequently been found to yield higher classification accuracies than MLC in the literatures (Kulkarni, 1998). Part of the reason may lie in the network design, that is, how many layers and nodes (neurons) the network requires to train the data, which can influences the classification results. Also, a study conducted by Vieira et al. (2000) showed that the ANN classifying the SPOT feature set resulted in lower overall kappa values than classifying the Landsat-TM feature set. It may be the nature of the feature set of SPOT, which is more difficult to classify using ANNs.

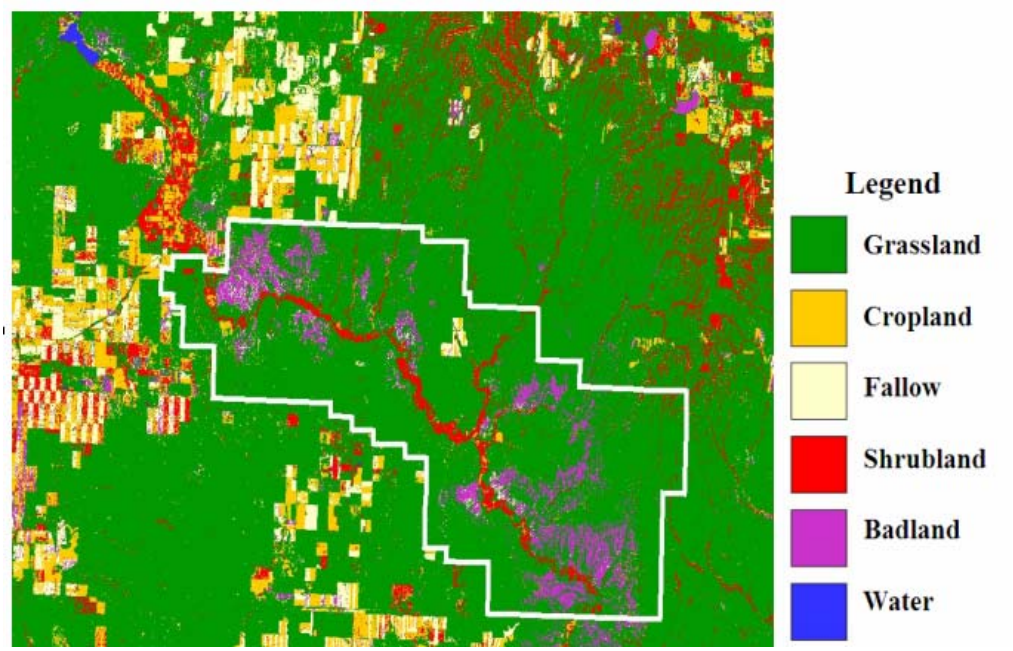

Figure 4-4 Land cover map generated from SPOT data using MLC for GNP.

4.4 Conclusions

The classification of land cover using SPOT remote sensing data is mostly controlled by the spectral variation within land cover classes and the spectral variation between classes. Knowledge of intra-class variation and inter-class variation is relevant to the accuracy of the final identification results.

In this study, three data sets and two classifiers were compared, in terms of their classification accuracy. An overall accuracy of 90.5% was obtained by MLC using Minnaert model transformed data. The results showed that MLC obtained better classification accuracy (~5%) than the back-propagation based ANN, topographic correction can reduce intra-class variation and improve classification accuracy at about 4% compared to the original reflectance, and the Minnaert model performed a slight higher classification accuracy (about 1%) than C-correction model. The improvement to

the classification from topographic correction on the SPOT data is not dramatic. Part of the reason may be the less solar zenith of the sensor and the relatively flat landscape in the study area. The vegetation indices, such as NDVI and ATSAVI, can contribute to the classification since they are sensitive either to green vegetation cover or to soil background. Spectral separability index (SSI) provides the analyst with a simple method to identify a subset of wavebands/vegetation indices to use in the classification. With regards to the ANN, it may be the nature of the SPOT data that leads to the lower classification accuracy comparing to the MLC.

Chapter 5 Discriminating invasive crested wheatgrass (*agropyron cristatum*) in northern mixed grass prairie using remote sensing technology

5.1 Introduction

Approximately one quarter of North America's remaining mixed-grass prairie lies within the Canadian Provinces of Alberta and Saskatchewan. Plants fix carbon and contribute most to the floral diversity and net primary productivity of the region (Andrew et al., 2003). However, invasive species, or non-native species, have threatened rare and endangered plant and animal species, and altered biodiversity and ecosystem function on the prairie (Bakker et al., 2003). Invasive species preempt native grass establishment and have been cited as the greatest obstacle to native grass restoration (Bakker et al., 2003). Invasive plant species result in economic and biologic detriment to rangeland and riparian ecosystems across the western United States and Canada. For instance, in the State of Idaho, the United States, $10 millions per year is spent in control measures alone. This estimate does not include economic impacts of invasive plants to regional industries such as agriculture and livestock, which cost over $137 billion per year in the U.S. (Lass et al., 2005).

Crested wheatgrass (*agropyron cristatum*) is a long-lived, cool season, introduced grass with extensive root systems, and is adapted to a wide variety of soils and can cope with severe drought stress (Hanks et al., 2005). This species can withstand weed competition and tolerate insect depredation. The biological and ecological characteristics of crested wheatgrass make it easily established in the cold, semiarid climate of the northern Great Plains (Asay et al., 1996). Large areas of abandoned croplands in the western U.S. were seeded with crested wheatgrass during the 1930's (Hanks et al., 2005). More than a million hectares were seeded with this species in both Montana and Canada prairie

(Hanks et al., 2005). Some of these communities have remained virtual monocultures for more than 50 years without apparent successional trends (Asay et al., 1999). The widespread crested wheatgrass has invaded native grassland and raised concerns regarding its ecological impact. Crested wheatgrass invasion of mixed-grass prairie was associated with lower diversity within and among plant communities, and appears to simplify the composition of mixed-grass prairie landscapes.

Figure 5-1 Crested wheatgrass (*agropyron cristatum*).

Crested wheatgrass is one of the major invasive species in the GNP. Monitoring the presence and spread of non-native species will be vital to help park managers control or remove the invasive species. In AFSC's rangeland insurance program, information of pasture types, such as native, improved or bush, was needed to assess the current year's yield. Therefore, mapping non-natives such as crested wheatgrass will assist AFSC to determine the acreages of different pasture types. Also, studying on the discriminating of crested wheatgrass represented the further classification of grasslands at species level after the land cover classification.

Traditionally, vegetation mapping and assessment techniques have been based primarily on field observation and data collection. Such mapping and assessment techniques are considered time-consuming, subjective, and always very limited in spatial extent

(Peterson et al., 2002). The use of the remotely sensed imagery has been demonstrated a cost-effective method to identify invasive species of grassland and their spread into the native grasslands. In contrast to field-based surveys, imagery can be acquired for all habitats, over a much larger spatial area, and in a shorter period of time (Underwood et al., 2003).

At the early stage of remote sensing development, large-scale aerial photographs were used to detect invasive plants (Havens et al., 1997; Kotschy et al., 2000; Krumscheid et al., 1998; Lathrop et al., 2003; Rice et al., 2000; Warren et al., 2001). In contrast to satellite imagery, aerial photography is capable of producing very high spatial resolution. Rowlinson et al. (1999) compared the accuracy of remote sensing data sources (aerial videography, aerial photography, and satellite imagery) for identifying and classifying alien invasive vegetation and concluded that the most accurate and cost-effective data source was panchromatic aerial photographs at a scale of 1/10,000. The major disadvantage for using aerial photography is that it is only feasible to collect data over a relatively small spatial area because of the high cost of image acquisitions and photo interpretation, and the interpretation of native and introduced species is problematic (Lass et al., 2005).

Facing the shortcomings with using aerial photography, more and more researchers have applied satellite-based imagery, mainly the hyperspectral and multispectral images, to detect invasive species from the native plants. The continuous nature of spectra inherent to hyperspectral imagery, such as AVIRIS and CASI, can be utilized to differentiate vegetation species because the large number of narrow wavebands is able to capitalize on both the biochemical and the structural properties of the target invader (Underwood et al., 2003). There have been a lot of studies using hyperspectral imagery to map invasive weed species such as leafy spurge (O'Neill et al., 2000), Brazilian pepper (Lass

et al., 2004), spotted knapweed (Lass et al., 2002), and yellow starthistle, and reached satisfactory accuracies (Lass et al., 2000). Mundt et al. (2005) used hyperspectral imagery to discriminate hoary cress in southwestern Idaho, USA, and obtained a maximum producer's accuracy of 82%. A study indicated that spotted knapweed was detectable using hyperspectral data when cover densities were greater than 70% and populations were larger than 0.1 ha (Lass et al., 2002). Glenn et al. (2005) applied HyMap hyperspectral data with a resolution of 3.5 m to detect leafy spurge, and demonstrated the ability of high resolution hyperspectral imagery to provide high quality data and consistent methods to locate small and low percent canopy cover occurrences of leafy spurge. These studies showed that hyperspectral sensors, especially with high resolution, could improve the ability to distinguish between vegetation species. Numerous investigators have also worked on developing techniques for using multispectral data in invasive species mapping and detection (Zhang et al., 2002; Vrindts et al., 2002). Peterson (2005) noted that *B. tectorum* cover was detectable from a single-date of Landsat Thematic Mapper (TM) imagery. The spatial resolution of the latest generation of satellites (e.g., IKONOS and Quickbird) can greatly advance detecting and mapping of invasive plant populations (Fuller, 2005). Although satellite imagery with higher spectral and spatial resolution can be available and mixing of reflectance signals can be avoided at a great extent, limited success has been achieved and invasive populations could not be detected if they were mixed with other vegetation or had not reached dominance (Lass et al., 2005).

Vegetation in different phenologies exhibits different spectral signatures. Most studies have utilized phenologically related measures (phenological differences between species) calculated from spectral vegetation indices to distinguish invasive species from native plants using multitemporal data and obtained satisfactory accuracy (Underwood et al, 2003; Egbert et al., 1997; Byeungwoo et al., 1999; Liu et al., 2002). Repeat images

acquired weeks to months apart provide an excellent method of exploiting phenological methods of discriminating species. However, combining images of multiple dates presents special challenges. Mis-registration or differences in illumination may limit the usefulness of multitemporal data sets especially if the data have only a limited number of spectral bands. Also, it may not be possible to collect cloud-free data during an optimal period.

Vegetation index (VI) is very useful for detecting invasive plants when they senesces before native vegetation. The NDVI is the most recognized vegetation index and has been successfully used to predict potential distribution of dyers woad (Lass et al., 2005) and to detect downy brome in rangeland (USGS, 2003). However, a fundamental problem with the VI approach for detecting species is its lack of generality. The debate over the optimal index of vegetation in arid lands is ongoing (Peterson, 2005). Due to similar cellular chemistry and architecture across species, vegetation reflectance is generally similar in the visible (VIS) and near-infrared (NIR) wavelengths (Cochrane, 2000), and absorption features for live vegetation are often overlapping (Schmidt et al., 2003). This situation makes it problematic to use vegetation indices to discriminate invasive species from native plants in a heterogeneous landscape (Lawrence et al., 2006). Therefore, accurate classification at species level is still difficult.

The principal challenges in using remote sensors to detect invasive species lie in the spectral similarity across species and invasive species often mixing with the native species. There does seem to be little information on the spectral properties of crested wheatgrass in the scientific literature and few studies have been conducted on using single-data SPOT to map crested wheatgrass in mixed prairie grasslands. The objectives of this study are (1) to assess the feasibility of discriminating crested wheatgrass in the mixed grass prairie using several potential vegetation indices derived from single-date

SPOT data and (2) develop a modified version of vegetation index that is expected to improve the separability in separating the invasive crested wheatgrass from native grasses.

5.2 Methods

5.2.1 Field data collection and remote sensing imagery

Field data collection was performed in later June and early July, 2005. A total of 261 point-based field samples were obtained and each field sample was located using a GPS (Garmine 76). The sample points were randomly selected from crested wheatgrass and native grassland, respectively. Cover percentage, dominant species, and topographic data were collected at each point. On each point, only one land cover type was included at the extent of 60 m from the point location. Field data were used as training sites and accuracy assessment of classification.

A SPOT 5 image (27 July, 2006) was used in this study, which covers the west block of GNP. The SPOT 5 image has 4 bands (Green, Red, NIR, and MIR) with a spatial resolution of 10 m. The imagery was georectified to a universal transverse Mercator (UTM) projection in order to match the field data. Over 30 GCPs and a DEM were used to correct distortions in raw images with satellite orbital modeling in order to increase the correction accuracy. The RMSE of the registration was controlled to be less than half pixel. The influence of the atmosphere degradation was removed and the digital number (DN) of the image was converted to reflectance by the radiometric correction (detailed methods see Chapter 2).

5.2.2 Vegetation indices selection

Finding a vegetation index that discriminates the species of interest from other species has been the focus of many studies (Baret et al., 1991; Broge et al., 2001; Haboudane et al., 2002). Even in the literature, the bands and indices used vary from one study to another. However, it was not the purpose of this study to evaluate the entire suite of vegetation indices reported in the literature; rather the focus was on a few selected indices that have shown to be good candidates for discriminating invasive species. Several broad-band vegetation indices, including normalized difference vegetation index (NDVI), normalized difference moisture index (NDMI), soil adjusted vegetation index (SAVI), modified soil adjusted vegetation index (MSAVI), simple ratio (SR), and triangulated vegetation index (TVI), were selected for this study based on their performance demonstrated in the previous studies (Davidson et al., 2003; Baret et al., 1989; Huete, 1988). These indices are based on either the combination of chlorophyll absorption band (red band) and NIR band located in the high reflectance plateau of vegetation canopies (NDVI, SAVI, MSAVI, and SR), or NIR and MIR band located within a region of water absorption (NDMI), or chlorophyll reflection band (green band) and chlorophyll absorption red band (TVI). The calculation formulation of these proposed vegetation indices are listed in Table 5-1 (L represents the soil reflectance factor; a constant of 0.5 was used for this study area).

Table 5-1 Vegetation indices used in discriminating crested wheatgrass.

VI	Formula	Reference
NDVI	$\frac{NIR - Red}{NIR + Red}$	Haboudane et al., 2004
NDMI	$\frac{NIR - MIR}{NIR + MIR}$	Labrecque et al., (2006)
SAVI*	$\frac{(1 + L) * (NIR - Red)}{NIR + Red + L}$	Haboudane et al., 2004
MSAVI*	$\frac{NIR - Red}{NIR + Red + L} * (1 + L)$	Tian et al., 1998
SR	$\frac{Red}{NIR}$	Stenberg et al., 2004
TVI	*0.5*(120*(NIR-Green))-(200*(Red-Green))*	Broge and Leblanc, 2000

* L=0.5 in the study area.

5.2.3 Modifying VI for discriminating crested wheatgrass

The classification of vegetation species using remote sensing data is mostly controlled by the spectral variation within species (intra-species) and the spectral variation between species (inter-species). However, the spectral separability between invasive and native species presents challenges for their accurate classification because the reflectance of vegetation from different species is usually very similar (Schmidt et al., 2003). The spectral separability is determined by the spectral mean differences between species and variation in the same species (Zhang et al., 2006). Numerous factors can lead to substantial spectral variance within species, including reflectance, absorption, and transmission properties of leaves and canopy, dead material, illumination, topography, and soil moisture (Zhang et al., 2006; He, et al., 2006). Some researchers have examined several methods, such as wavelet transformation and derivative analysis, for reducing spectral variation within species (Zhang et al., 2006). Although the derivative of

reflectance spectra has been applied to reduce background signals and enhance subtle spectral features in detection of vegetation species, some results suggest that it may not be optimal for species identification in using hyperspectral data because it does not effectively decrease the spectral variation within species (Zhang et al., 2006). Zhang et al. (2006) found that wavelet transformation could be capable of reducing variation within species at a coarse scale of wavelet coefficients and could be a very useful tool for species identification. However, wavelet coefficients at fine scales may not be informative for the purpose of identification of vegetation species, and wavelet analysis could not enlarge inter-class variability among classes. Thus, a more global view of reflectance may be more useful for the identification of vegetation species than simply observing the reflectance at finely resolved spectral bands. Also, the specific wavelet features and scale may vary for different species and ecosystems (Zhang et al., 2006).

By examining the spectral curves it was found that the largest difference between crested wheatgrass and natives occurred in NIR and MIR bands. It meant that NDMI, which is calculated from the two bands, may be a promising variable to separate the two vegetation types. NDMI has proven to be a better greenness measure and showed less saturation effects when the LAI /living biomass reaching higher level (Saltz et al., 1999). However, the difference of NDMI between the two vegetation types is limited and not large enough to distinctly separate crested wheatgrass and native grasses because of higher variances. For the purpose of reducing intra-class variations and enlarging inter-class difference, an adjustment factor (L) was incorporated to enlarge the difference among classes; further, an exponential transformation was performed upon the modified index to suppress the variations within class. The exponential NDMI is formulated as follows (Equation 5-1):

$$\text{ExpNDMI} = Exp\left(\frac{\text{MIR} - \text{NIR}}{\text{MIR} + \text{NIR} - L}\right) \quad (5\text{-}1)$$

The difference of ExpNDMI between classes increases with an increase in adjusting factor L, while the intra-class variation also increases, in spite of their different increasing rates (Figure 5-2). In order to get the optimal L value, SSI (detailed information on SSI was described in Chapter 3) was applied to assess the spectral separability. A higher inter-class variability and smaller intra-class variability will result in a larger SSI value. The larger the SSI value, the better the spectral separability. In this study, adjustment factor *L* was changed from 0 to 0.4 at an interval of 0.01 to investigate the relationship between the difference of classes and the variations in classes using the spectral data within training area, and found $L = 0.2$ to be the optimal adjustment value that obtained the largest SSI (Figure 5-3).

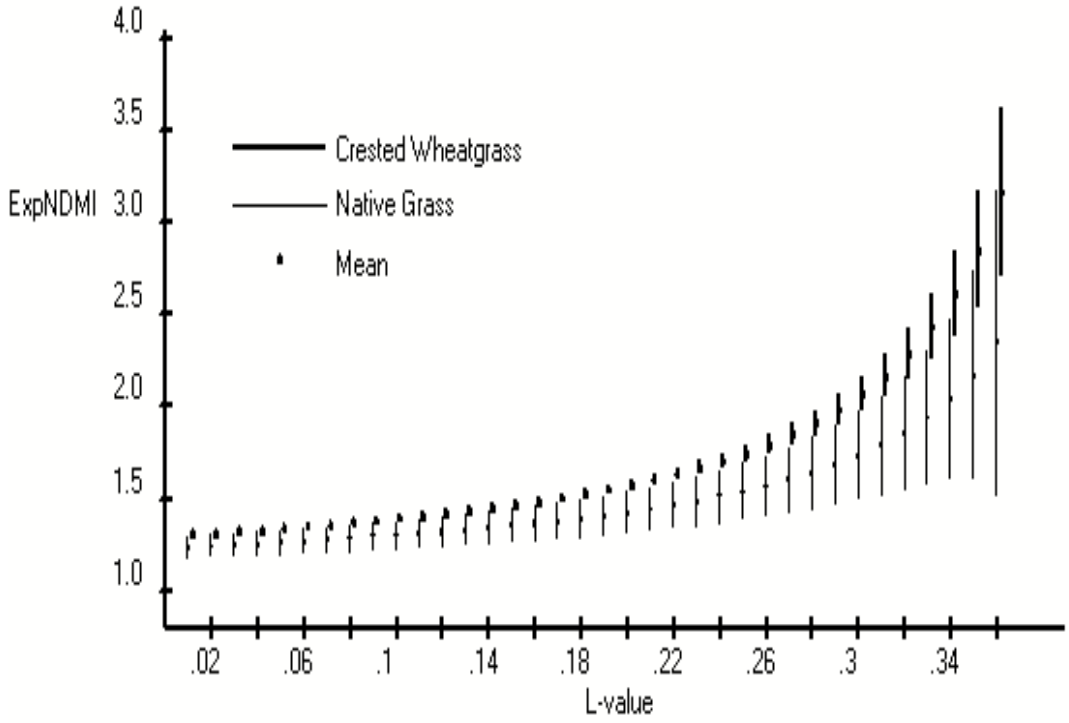

Figure 5-2 Average ExpNDMI + 1 SD (standard deviation) for crested wheatgrass and native grasslands *vs* the change of adjustment factor *L*.

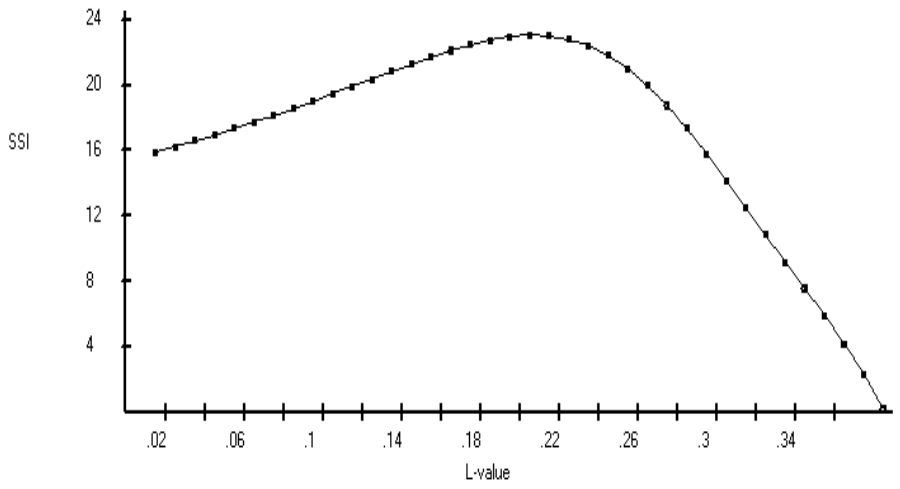

Figure 5-3 Spectral separability index (SSI) *vs* adjusting factor L. Higher SSI value indicates the better separability between native grasslands and crested wheatgrass.

5.2.4 Statistic feature analysis

Initial analyses of the reflectance spectra, including the calculations of the mean, standard deviation in all bands and VIs, were done on the two classes using the extracted reflectance based on the training sites. Because the classification accuracy mainly depends on the spectral difference among classes, the analysis was focused on the spectral separability of each band or VIs on the two classes. The aforementioned SSI was applied to assess the ability of each band or VI in distinguishing the vegetation species. Band or VI with low separability was excluded in the classification.

5.2.5 Band selection, classification, and accuracy assessment

The point-based field data (94 points) were used as training sets for the two classifiers. Each point was buffered by 20 meters to represent the four pixels of SPOT 5 imagery. Given a number of bands of remotely sensed data and their transformations (e.g.,

vegetation index), it would require a complex algorithm to identify, from all the possible combinations, the best band combination for classification. In this study, the bands or vegetation indices were selected as inputs for classification based on their spectral separability. Bands or VIs with larger SSI value were selected.

In view of the facts that, based on the preliminary analysis, the intra-class spectral variation did not follow a normal distribution and the homogeneity of variances assumption was not met for the crested wheatgrass, an artificial neural network (ANN) classifier based on back propagation (BP) algorithm was employed to classify crested wheatgrass and native grasslands in this study. The advantage of ANN is that no prior statistical information is needed about the input data, and makes no assumptions about the nature of the data distribution (Kulkarni, 1998). The effectiveness of artificial neural networks to solve highly non-linear problems such as land-cover classification based on multispectral imagery has been demonstrated (Mutanga et al., 2004).

In order to investigate the ability of ExpNDMI in discriminating crested wheatgrass from native grasslands, classifications using band combinations with ExpNDMI and without ExpNDMI were tested with BP based ANN. Also, an unsupervised automated classification method was applied first to generate a grasslands “mask” for further classification of crested wheatgrass and native grassland, which might reduce the calculation time and the uncertainty of classification caused by other land covers.

A total of 167 point based samples were used in post-classification accuracy assessment. Three types of accuracies were calculated (overall accuracy, producer’s accuracy, and user’s accuracy) and compared for different band/VIs combinations.

5.2.6 Outline of research method

Figure 5-4 depicts the methods and procedures that applied SPOT 5 data to discriminate crested wheatgrass from natives in the study area.

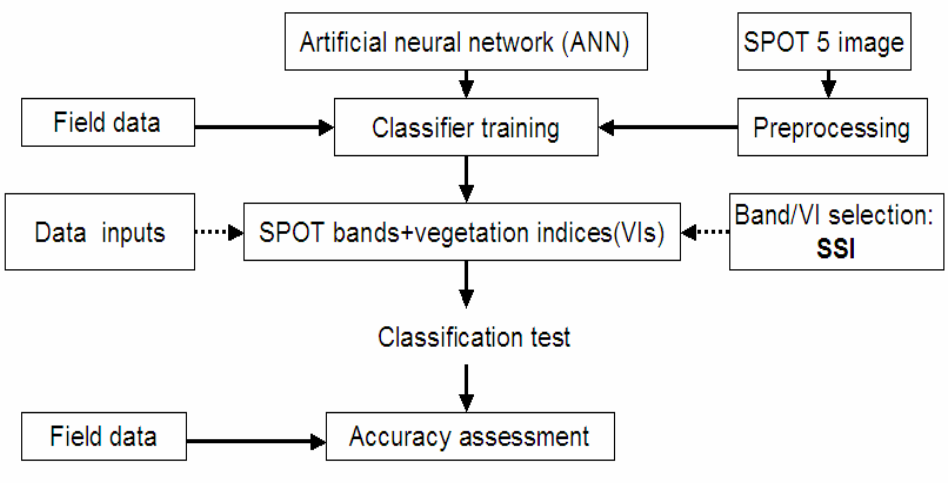

Figure 5-4 Flow chart for discriminating crested wheatgrass using SPOT data.

5.3 Results and discussions

5.3.1 Spectral separability between native grasslands and crested wheatgrass

Figure 5-5 shows atmospherically corrected reflectance of native grasslands and crested wheatgrass by four SPOT bands and different VIs. Similar spectral patterns were found for the two vegetation types, e.g., higher reflectance in the NIR band and lower reflectance in the red band. On average, crested wheatgrass has lower reflectance in all bands comparing to native grasslands, despite the occurrence of a very small difference in the MIR band. This may be due to the lower photosynthetic rates and stomatal conductance of crested whatgrass than the native grasses in the summer months (Nowak et al., 1986), in which the image was acquired. Crested wheatgrass is a cool season plant,

and it tends to go semi-dormant during midsummer months. The spectral reflectance features of crested wheatgrass and native grasslands may reflect phenological and compositional differences in the vegetation. Comparing to native range, there are more abundant senesced vegetation in crested wheatgrass pastures (e.g., litters. He, et al., 2006) that probably contributes to the lower reflectance (Thomson et al., 1990). Also, crested wheatgrass has rougher surface than native species, which may lead to the lower reflectance.

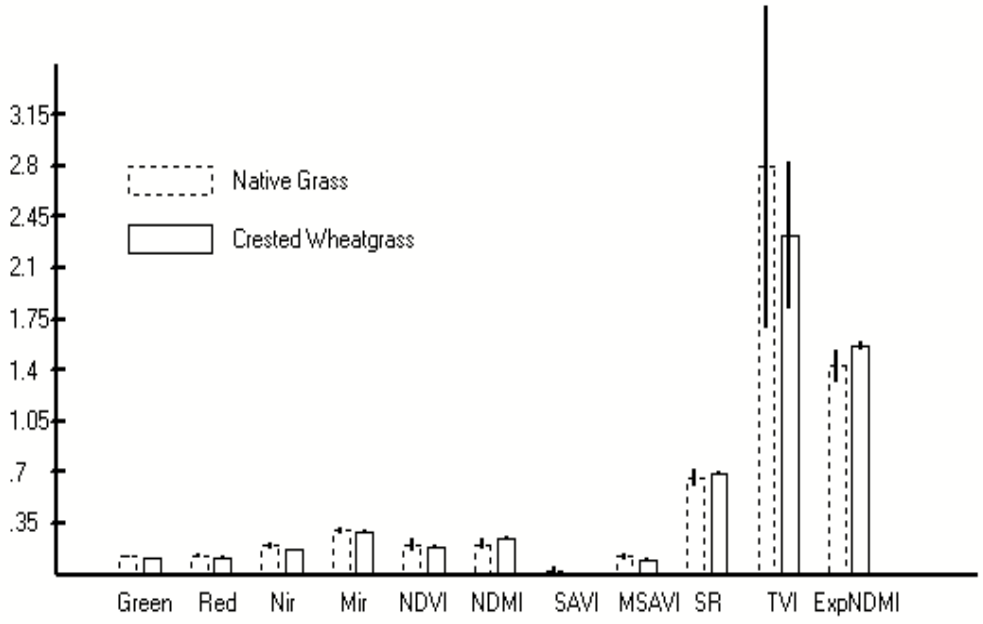

Figure 5-5 Reflectance/VI mean and 1st SD (Standard Deviation, indicated in bold line) in SPOT bands and VIs for crested wheatgrass and native grasslands.

With regard to the differences between single bands for the two classes of vegetation, the greatest reflectance difference was found in the NIR (Figure 5-5) and it shows the maximum spectral separability in the four SPOT bands (Figure 5-6). Green band also showed better separability in comparison with red and MIR bands. This may be due to the fact that the green band to be more sensitive than the red band in detecting leaf chlorophyll variation. Differences between the two vegetation types in the NIR band

may be due to their differences in plant photosynthetic rates; NIR wavelengths are more reflected by healthy, photosynthetically active vegetation, while crested wheatgrass has lower photosynthetic rates in the midsummer (Nowak et al., 1986). NDMI, which is calculated from NIR and MIR, showed the highest separability between native grassland and crested wheatgrass among the initially selected VIs. This is due to the greatest spectral difference in the NIR and similar reflectance in MIR for the two vegetation types. The limited success of other indices is related to the fact that the reflectances in all bands are similar for the two vegetation types. The ExpNDMI, which is modified from NDMI, exhibits the largest separability among the VI group and all single SPOT bands. Compared to the NDMI, ExpNDMI greatly increased the spectral separability because it significantly reduced the intra-species variation and enlarge the inter-species variation. It would be expected to increase the classification accuracy of invasive crested wheatgrass and natives. Some VIs, such as TVI, revealed significant overlap in the spectral space, and therefore, reached very lower separability in discriminating crested wheatgrass from natives. Separablity had helped in selecting proper bands and VIs to be included in the classification of crested wheatgrass. Bands or VIs with lower separability were excluded from the classification inputs.

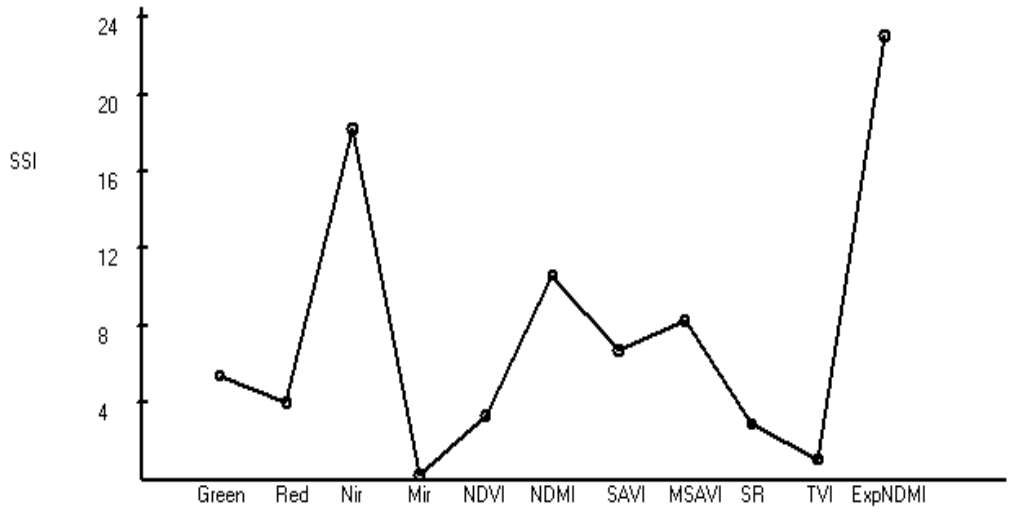

Figure 5-6 SSI for SPOT bands and VIs in discriminating crested wheatgrass from native grasses.

5.3.2 Classification and accuracy assessment

Based on the spectral separability analysis, bands and vegetation indices were selected for which the native grasses and crested wheatgrass were spectrally different. The classification was performed using two combinations: one with the SSI greater than 4.0 (including Green, NIR NDMI, SAVI, MSAVI, and ExpNDMI) and another with the SSI greater than 8.0 (including NIR, NDMI, MSAVI, and ExpNDMI). An artificial neural network (ANN) classifier based on back propagation (BP) algorithm was applied to classify crested wheatgrass and native grasslands. One input Layer (2 nodes for per channel), two hidden Layer (8 nodes for per layer), and one output Layer (2 nodes) were designed for the neural network, and sigmoid function was used as activation function. For the purpose of investigating the performance of ExpNDMI in the discriminating crested wheatgrass, another two combinations were tested: one with ExpNDMI (Green,

NIR, SAVI, MSAVI, and ExpNDMI) and another without ExpNDMI, which was substituted by NDMI (Green, NIR, SAVI,MSAVI, and NDMI).

An evaluation of classifications using increasing numbers of bands and VIs showed an improvement in overall classification accuracy and overall kappa (Table 5-2).

Table 5-2 Classification accuracy for different combinations.

Band/VI combinations		Producer's accuracy	User's accuracy	Overall Accuracy	Overall Kappa
Green, NIR, NDMI	Natives	81.1%	85.1%	79.4%	0.568
SAVI, MSAVI,	CW*	76.6%	75.0%		
ExpNDMI					
NIR, NDMI, MSAVI	Natives	86.8%	80.7%	78.8%	0.537
ExpNDMI	CW	65.6%	71.0%		
Green, NIR, SAVI,	Natives	82.1%	81.3%	77.1%	0.510
MSAVI ExpNDMI	CW	68.8%	69.8%		
Green, NIR, NDMI,	Natives	82.1%	76.3%	72.9%	0.409
SAVI MSAVI	CW	57.8%	66.1%		

* CW=crested wheatgrass.

Combination of Green, NIR, NDMI, SAVI, MSAVI, and ExpNDMI obtained the highest overall accuracy of 79%. This suggests that the adding of more layers with higher separability could capture more spectral feature of interested targets and contribute the improvement of classification. However, inclusion of too many additional bands/VIs with lower separability will lead to inconsistent classification criteria and unreliable results. The misclassification between natives and crested wheatgrass could be attributed to many factors, the major one of which could be the spectral similarity between the two

vegetation types. Although SPOT 5 image with higher spatial resolution was applied in this study, its lower spectral resolution could not discern the subtle difference between the two vegetation types, especially when they are mixed with each other.

The result of classification using combination with ExpNDMI layer showed that ExpNDMI improved the classification accuracy by more than 4% of overall accuracy than the combination without ExpNDMI. This result indicates that ExpNDMI is much better to reflect the spectral difference between crested wheatgrass and native grasslands than NDMI. ExpNDMI had the highest separability among all the bands and VIs because it can significantly suppress the intra-class variation and enlarge the inter-class variation.

A visual inspection of the crested wheatgrass classification map (Figure 5-7) indicates that the crested wheatgrass was over-classified, especially in the low-left of the map. This may be due to the reflectance of plants in this area to be very similar to that of the crested wheatgrass community. This result is consistent with the previous studies that indicated that there is a tendency for the invasive species to be over-classified, that is, more pixels are identified as invasive species than actually exist (Lass et al., 2002).

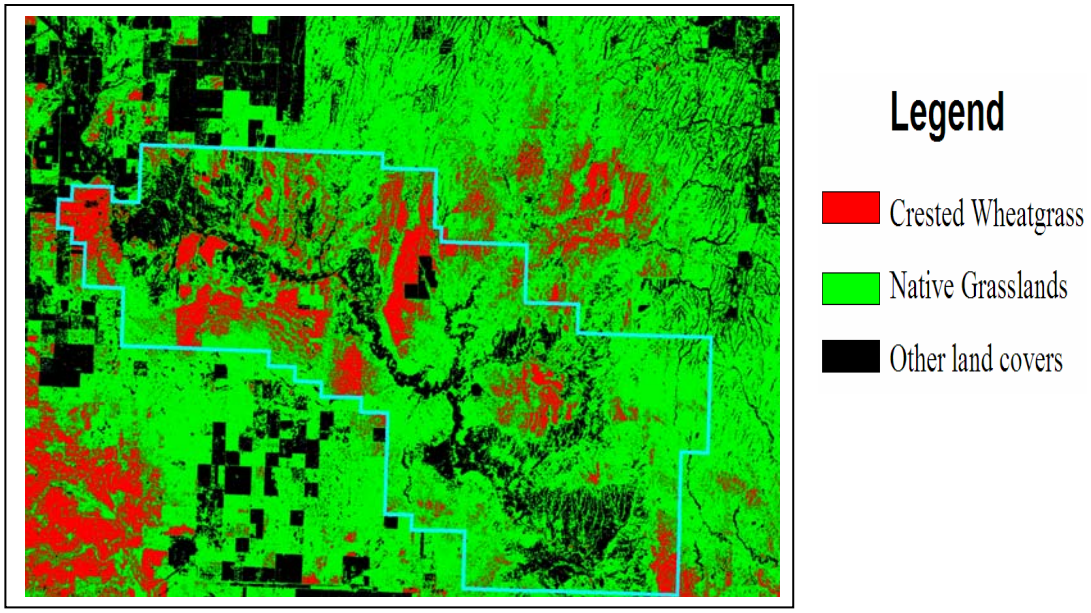

Figure 5-7 Crested wheatgrass classification map.

A digital vegetation map of the GNP region from Parks Canada was acquired. This map was only created for lands within the GNP boundary for which the park held title in 1993. The inventory was initiated to fulfill requirements of the GNP resource management program, particularly the formulation and implementation of a management plan for the park. The resulting vegetation map was based on the interpretation of 1:12,500 scale airphotos (collected 1982) and a subsequent intensive field survey (carried out in 1993). By comparing the classifying map (Figure 5-7) with the previous digital vegetation map, there was a striking difference between the two maps. There had been a great expansion of crested wheatgrass since the previous digital vegetation map was made, in spite of the fact that the crested wheatgrass was over-classified in this study.

5.4 Conclusions

In this research several selected vegetation indices were assessed in discriminating

crested wheatgrass from natives in mixed grass prairie. The results showed that the single-date SPOT 5 image used in this study obtained 79% of overall accuracy in separating crested wheatgrass, and the proposed ExpNDMI can reduce intra-species variation and enlarge inter-species variation, and, further, improve the ability to discriminate invasive crested wheatgrass from natives at 4% of overall accuracy. However, the crested wheatgrass was over-estimated in this study, and the result indicated that single-date SPOT 5 image could not separate the crested wheatgrass from natives with satisfactory accuracy. The reason may be due to the spectral similarity between natives and crested wheatgrass. It can be speculated that the accuracy may be improved with a multi-temporal approach, especially an image from early spring. Results of this study demonstrated that the selected vegetation indices in this study have limitations in discriminating the two plant types, and the ExpNDMI developed in this study obtained much better separability than other selected VIs for the two grass types and could increase classification accuracy of crested wheatgrass and native grasslands to some extent in the study area.

Since vegetation reflectance depends on a complex interaction of several internal and external factors that may vary greatly in time and space and from one species to another, no universal spectral pattern between two vegetation species can be expected to exist. Consequently, this pattern will be site-, time- and species-specific, and therefore not directly applicable for large-scale operational use. Although higher spatial and spectral resolution is desirable in order to avoid mixing of reflectance signals originating from different vegetation types, the spectral similarity at species level is still the greatest challenge in discriminating invasive species. Therefore, the methods and the new vegetation index, ExpNDMI, developed in this research were limited to certain physical and biological conditions which are similar to this study area.

Chapter 6 Summary

This study applied multispectral SPOT imagery with medium resolution (20 and 10 m), field collected data, and GIS data to investigate the classification techniques of land cover and vegetation at species level. Two topographic correction models, Minnaert model and C-correction, were assessed, and two classifying algorithms, maximum likelihood classifier (MLC) and artificial neural network (ANN), were evaluated. The feasibility of discriminating invasive crested wheatgrass from natives was examined. The purposes were to explore the feasible approaches to update the land cover data for implementing a rangeland insurance program.

6.1 Conclusions

Two topographic correction models, Minnaert constant and C-correction, were tested, and the results showed that the two models could be effective to reduce radiometric variation among land cover classes caused by topographic effect on the SPOT image in the study area. The topographic corrections achieved better intra-class homogeneity within land cover classes and improved the classification. The results demonstrated the usefulness of the topographic correction in land cover classification in the study area featured by gently rolling hills. However, the two topographic corrections applied in this study did not obtain significant reduction in variations within the interested land cover classes. Part of the reason may be the less solar zenith of the sensor, relatively flat terrain in the study area, and the inappropriate samples for estimating the Minnaert constants and C coefficients.

Two classifiers, MLC and ANN, were tested and compared by using the original reflectance, corrected reflectance from the two topographic correction models, and corresponding VIs derived from the three data sets as inputs to the classifiers, in terms

of classification accuracy. An overall accuracy of 90.5% was obtained by MLC using Minnaert model corrected reflectance of SPOT image. The results showed that MLC obtained 5% of classification accuracy more than the back-propagation based ANN. The reason may lie in the nature of the feature set of SPOT image, which is more difficult to classify using ANN. Topographic correction can reduce intra-class spectral variation and improve classification accuracy by about 4% compared to using original reflectance; significant, although not dramatic.

Classification using remote sensing data at species level faces many difficulties at present. The major challenges lie in the facts that spectral features among species are similar in remote sensing data with broadband, and invasive species often mix with natives. In this research, several selected vegetation indices and a new vegetation index developed in this study were assessed using a spectral separability index (SSI). The single-date SPOT 5 image with a resolution of 10 m obtained 79% of overall accuracy in discriminating crested wheatgrass from natives. The proposed ExpNDMI can greatly reduce intra-class variation and enlarge inter-class variation, so as to improve the ability to discriminate invasive crested wheatgrass from natives at 4% of overall accuracy. By examining the classification map, however, it was found that the crested wheatgrass was over-estimated in this study; the reason may lie in the spectral similarity between natives and crested wheatgrass. The result indicated that single-date SPOT 5 image could not separate the crested wheatgrass from natives with satisfactory accuracy. It can be speculated that the accuracy can be improved with a multi-temporal approach, especially using images from early spring. Results of this study demonstrated that the selected vegetation indices in this study have limitations in discriminating the two plant types, and the proposed ExpNDMI received much better separability than other selected VIs for the two grass types and could improve the classification of crested wheatgrass and native grasslands in the study area.

In conclusion, remote sensing can be a reliable approach to update land cover information for implementing a rangeland insurance program by using a single-date multispectral imagery with medium resolution.

6.2 Significances

Land cover mapping provides key information needed for resource management and policy development, represents an important baseline for environmental and habitat monitoring, scientific analyses, and serves as inputs in modeling of biogeochemistry, carbon cycle, hydrology, and climate change. Land cover data have an auxiliary role to estimate other surface variables. Undoubtedly, it is important to further study mapping land cover by remote sensing.

This study provides an accurate and cost-effective approach to map land cover using single-date remote sensing images and make it technologically feasible for insurance corporations to implement a rangeland insurance program in the prairie. The techniques proposed in this study can be applied in similar ecosystems. The generated land cover/species classification map can be used in many fields as mentioned above. For example, the insurance corporation can overlay the classification map and the digital township boundaries to calculate the acreages of different land covers/pasture types for each township. This spatial analysis will assist insurance companies in verifying the acreages of pasture types for which the ranchers apply for participating in a rangeland insurance program in order to combat insurance fraud and abuse. Also, classification map provides a basis for yield calculation for different pasture types. Pasture yield is highly related to its types. Based on different pasture types, we can obtain more accurate information on the relationship between pasture yields and satellite imagery data.

Techniques using single date satellite image to map land cover in the mixed grasslands were investigated in this study. It may lessen the dependence on the multitemporal data, which may be difficult, if not impossible, to obtain cloud-free image during an optimal season for land cover classification. In addition, a proposed vegetation index, ExpNDMI, was developed and demonstrated to be effective in enhancing the separability between crested wheatgrass and natives in this study, and it may provide researchers with an alternative method in separating plant species. Also, the results of this research showed that the topographic correction can reduce spectral variation within specific land cover class and improve the classification to some extent, even in areas with gentle slopes. This suggest a new idea that topographic correction may be necessary before performing classification in gentle rolling hills, although some researchers believe that the effect of topography can be ignored if the slope is not too steep (Combal, B. and Isaka, H. 2002)

6.3 Limitations

This study discussed the classification of land cover and plant species using single-date image in the mixed grasslands. However, there are some limitations with this study. Due to the lack of appropriate ground collected spectral data and spectral libraries for the study area, the topographically corrected data were not compared with the ground truth in order to assess the effectiveness of topographic correction. It is not certain how well the topographic effect was removed. Another limitation is the number of the spectral bands for SPOT is limited (it only cover four bands in the visible and infrared range), thus, there was no flexible option to select proper bands in order to accurately separate land cover classes and species. Also, since only the single-date image were used in this study, the phenological difference between crested and natives could not be applied in the analysis, and consequently, crested wheatgrass could not be classified with satisfactory accuracy. In addition, the optimum spatial resolution for land cover classification in the high heterogeneous mixed grasslands was not investigated because

of the lack of remotely sensed data with different spatial resolution.

6.4 Recommendations for future studies

Further studies are still needed in order to obtain better results for the land cover and species classification using remotely sensed data. For future researches, field spectral data close to the dates of the satellite overpasses should be collected in order to support and validate the topographic correction. Parameters of topographic correction models can be calculated within each land over class or by establishing a random coefficient model that allows the parameters to vary across subjects (i.e., slope/aspect classes). It can be speculated that using parameters calculated by the above methods may improve topographic correction and, further, improve the classification because spectral variation within classes may be reduced more significantly. Also, multitemporal data should be tested to identify the spectral signatures of land cover classes and vegetation species in different phenologies. It is expected that the application of the phenologically related measures (phenological differences between land cover classes or species) can improve the classification by using multitemporal remotely sensed data. In addition, the use of hyperspectral and multi-sensor data should be investigated in order to identify optimal bands and resolution applied in the land cover classification in the more diversified mixed grasslands.

References

Adams, R. M., Hurd, B. H., Lenhart, S. and Leary, N., 1998, Effects of global climate change on agriculture. *Climate Research,* Vol. 11, pp. 19–30.

AFSC, 2002, Annual report 2001-2002.

AFSC, 2003, Annual report 2002-2003.

AFSC, 2005, Annual report 2004-2005.

Asay, K.H., Jensen, K.B., Horton, W.H., Johnson, D.A., Chatterton, N.J. and Young, S.A., 1999, Registration of 'RoadCrest' crested wheatgrass. *Crop Sci.,* 39, pp. 1535-1546.

Asay, K.H. and Jensen. K.B., 1996. The wheatgrasses-cool-season grasses. *Agron. Monorg,* 34. pp. 221-235.

Atwood, J., Watts, T., Price, K. and Kastens, J., 2005, The big picture─satellite remote sensing applications in rangeland assessment and crop insurance. *Proceedings, Agricultural Outlook Forum,* 24 February, 2005, Arlington, Virginia. Speech Booklet 2, pp 26-52.

Atzberger, C., 2004, Object-based retrieval of biophysical canopy variables using artificial neural nets and radiative transfer models. *Remote Sensing of Environment,* Vol.93, Issue 1-2, pp 53-67.

Bakker, J.D., Wilson, S. D., Christian, J. M. and Li, X., 2003, Contingency of grassland restoration on year, site and competition from introduced grasses. *Ecological Applications,* 13(1), pp. 137–153

Baret, F., Guyot, G., and Major, D.J., 1989, TSAVI: a vegetation index which minimizes soil brightness effects on LAI and APAR estimation. In *IGARSS '89, Proceedings of the IEEE International Geoscience and Remote Sensing Symposium and 12th Canadian Symposium on Remote Sensing*, 10–14 July 1989, Vancouver, B.C. IEEE, Piscataway, N.J. Vol. 3, pp. 1355–1358.

Benediktsson, J. A., Sveinsson, J. R., Swain, P. H., 1997, Hybrid consensus theoretic classification. *IEEE Transactions on geoscience and remote sensing,* Vol. 35, No. 4, pp. 833-843.

Bischof, H., Schneider, W. and Pinz, A. J., 1992, Multispectral classification of Landsat-images using neural networks, *IEEE Trans. Geosci. Remote Sensing.,* 30 (3), pp. 482-490.

Bishop, C. M., 1995, Neural networks for pattern recognition. New York, NY USA, Oxford University Press.

Boles, S. H., Xiao, X., Liu, J., Zhang, Q., Munkhtuya, S., Chen, S. and Ojima, D., 2004, Cover characterization of temperate east Asia using multi-temporal VEGETATION sensor data. R*emote Sensing of Environment.* 90. pp. 477–489.

Bostater, C. R., Ghir, T., Bassetti, L., Hall, C., Reyeier, E., Lowers, R., Holloway-Adkins, K. and Virnstein, R., 2004, Hyperspectral remote sensing protocol development for submerged aquatic vegetation in shallow waters. *Proc. SPIE Int. Soc. Opt. Eng.* 5233, pp. 199–215.

Broge, N. H. and Leblanc, E., 2000, Comparing prediction power and stability of broadband and hyperspectral vegetation indices for estimation of green leaf area index and canopy chlorophyll density. *Remote Sensing of Environment,* 76, pp. 156-172.

Bruce, L. M., Li, J. and Huang, Y., 2002, Automated detection of subpixel hyperspectral targets with adaptive multichannel discrete wavelet transform. *IEEE Transactions on Geoscience and Remote Sensing*, 40, pp. 977−980.

Bruzzone, L., Cossu, R. and Vernazza, G., 2002, Combining parametric and non-parametric algorithms for a partially unsupervised classification of multitemporal remote sensing images. *Information Fusion,* 3, pp. 289-297.

Byelingwoo, J. and Landgrebe, D.A., 1999, Decision fusion approach for multitemporal classification. *IEEE Transactions on Geoscience and Remote Sensinf;*. 37,

pp.1227-1233.

Carmel, Y. and Kadmon, R., 1998, Computerized classification of Mediterranean vegetation using panchromatic aerial photographs. *Journal of Vegetation Science*, 9 (3), pp. 445-454.

Chang, C. and Wang, S., 2006, Constrained Band Selection for Hyperspectral Imagery. *IEEE Transactions on geoscience and remote sensing,* Vol. 44, No. 6, pp. 1575-1585.

Chomentowski, W., Salas, B. and Skole, D., 1994, Landsat pathfinder project advances deforestation mapping. *GIS World*, 7, pp.34– 48.

Cihlar, J., Xiao, Q., Chen, J., Beaubien, J., Fung, K.and Latifovic, R., 1998, Classification by progressive generalization: A new automated methodology for remote sensing multichannel data. *International Journal of Remote Sensing*, 19, pp. 2685–2704.

Cingolani, A. M., Renison, D., Zaka, M. R. and Cabido, M. R., 2004, Mapping vegetation in a heterogeneous mountain rangeland using landsat data: an alternative method to define and classify land-cover units. *Remote Sensing of Environment,* 92, pp. 84–97.

Civco, D. L., 1989, Topographic normalization of Landsat Thematic Mapper digital imagery Photogramm. *Eng. Remote Sens.,* Vol. 55, pp. 1303–1309.

Cochrane, M. A., 2000, Using vegetation reflectance variability for species level classification of hyper spectral data. *Int'l J. Remote Sensing,* 21(10), pp. 2075-2087.

Cohen, Y. and Shoshany, M., 2005, Analysis of convergent evidence in an evidential reasoning knowledge-based classification. *Remote Sensing of Environment,* 96, pp. 518 – 528.

Colby, D. J., 1991, Topographic normalization in ragged terrain. *Photogrammetric Engineering and Remote Sensing*, 57, pp. 531–537.

Combal, B. and Isaka, H., 2002, The effect of small topographic variations on reflectance. *IEEE Transactions on geoscience and remote sensing,* Vol. 40, No. 3*,* pp. 663-670.

Conese, C., Gilabert, M. A., Maselli, F. and Bottai, L., 1993, Topographic normalization of TM scenes through the use of an atmospheric correction method and digital terrain models, *Photogramm. Eng. Remote Sens.*, Vol. 59, No. 2, pp. 1745–1753.

Davidson, A. and Csillag, F., 2003, A comparison of three approaches for predicting C4 species cover of northern mixed grass prairie. *Remote Sensing of Environment,* 86, pp. 70–82.

DeFries, R., Hansen, M. and Townshend, J., 1995, Global discrimination of land cover types from metrics derived from AVHRR pathfinder data. *Remote Sens. Environ.*, Vol. 56, pp. 209–222.

Dymond, J. R. and Shepherd, J. D., 1999, Correction of the topographic effect in remote sensing. *IEEE Transactions on geoscience and remote sensing,* Vol. 37, No. 5, pp. 2618-2620.

Ekstrand, S., 1996, Landsat TM-based forest damage assessment:correction for topographic effects. *Photogrammetric Engineering and Remote Sensing,* 62, pp. 151–161.

Goodwin, B. K., Vandveer, M. L. and Deal, J. L., 2004, An empirical analysis of acreage effects of participation in the federal crop insurance program. *American Journal of Agriculture Economics,* 86(4), pp. 1058-1077.

Egbert, S., Lauver, C., Blodgett, C , Price, K. and Martinko, E., 1997, Mapping the Kansas grasslands: A multiseasona! approach. *GAP Analyxis Bullciin,* 6, pp. 12-13.

Erbek, F. S., Ozkan, C. and Taberner, M., 2004, Comparison of maximum likelihood classification method with supervised artificial neural network algorithms for land use activities. *International Journal of remote sensing,* Vol. 25 Issue 9, pp.

1733-1749.

Feng, J., Rivard, B. and Sanchez-Azofeifa, A., 2003, The topographic normalization of hyperspectral data: implications for the selection of spectral end members and lithologic mapping. *Remote Sensing of Environment*, 85, pp. 221–231.

Franklin, S. E., Lavigne, M. B. and Hunt, E. R., Jr., 1995 Topographic dependence of synthetic aperture radar imagery. *Comput. Geosci.* 21(4), pp. 521–532.

Franklin, S. E., Stenhouse, G. B., Hansen, M. J., Popplewell, C. C., Dechka, J. A.and Peddle, D. R., 2001, An integrated decision tree approach(IDTA) mapping landcover using satellite remote sensing in support of Grizzly Bear Habitat analysis in the Alberta Yellowhead Ecosystem. *Canadian journal of remote sensing,* Vol. 27, No.6, pp. 579-592.

Fuller, D. O., 2005, Remote detection of invasive Melaleuca trees *(Melaleuca quinqucnevvia)* in south Florida with multispectral IKONOS imagery. *International Journal of Remote Sensing,* Vol. 26, No. 5, 10,pp. 1057-1063.

Giri, C., Zhu, Z. and Reed, B., 2005, A comparative analysis of the Global Land Cover 2000 and MODIS land cover data sets. *Remote Sensing of Environment.* 94, pp.123–132.

Glenn, N. F., Mundt, J. T., Weber, K. T., Prather, T. S., Lass, L. W. and Pettingill, J., 2005, Hyperspectral data processing from repeat detection of small infestations of leafy spurge. *Remote Sensing of Environment,* 95, pp. 399– 412.

GNP annual report, 1997.

Goodwin, B. K., Vandveer, M. L. and Deal, J. L., 2004, An empirical analysis of acreage effects of participation in the federal crop insurance program. *American Journal of Agriculture Economics*, 86(4), pp. 1058-1077.

Goyal, S. K., Seyfried, M. S. and O'Neill P. E., 1999, Correction of surface roughness and topographic effects on airborne SAR in mountainous rangeland areas. *Remote Sensing of Environment.* 67, pp. 124–136.

Guo, X. and Richard, P., 2004, Assessing Canadian prairie drought with satellite and climate data. *Environmental Informatics Archives*, Vol 2, pp. 422-430.

Haboudane, D., Miller, J.R., Pattery, E., Zarco-Tejad, P.J., Strachan, I.B., Labrecque, S., Fournier, R.A., Luther, J.E. and Piercey, D., 2006, A comparison of four methods to map biomass from Landsat-TM and inventory data in western Newfoundland. *Forest Ecology and Management.* 226, pp 129–144.

Hanks, J. D., Waldron, Blair L., Johnson, P. G., Jensen, K. B. and Asay, K. H. 2005, Breeding CWG-R Crested Wheatgrass for Reduced-Maintenance Turf. *Crop Sci.* 45, pp. 524–528.

Havens, K.J., Walter, I. and Berquist, H., 1997, Investigation and long-term monitoring of *Phragmites australis* within Virginia's constructed wetland sites. *Environmental Management,* 21, pp. 599-605.

Hayes, M. J., Svoboda, M. D., Knutson, C. L. and Wilhite, D. A., 2004, Estimating the economic impacts of drought. *American Meteorological Society. 14th Conference on Applied Climatology, Joint Session 2, 84th American Meteorological Society Annual Meeting, 10-16 January 2004; Seattle, Washington.* 3 pp.

He, Y., Guo, X. and Wilmshurst. J., 2006, Studying mixed grassland ecosystems suitable hyperspectral vegetation. *Can. J. Remote Sensing*, Vol. 32, No. 2, pp. 98–107.

Hejmanowska, B., 1998, Removal of topographical effect from remote sensing data for thermal inertia modeling. *IAPRS,* Vol. 32, Part 4 "GIS-Between Visions and Application", Stuttgart, pp. 238-246.

Hill, M. J., Vickery, P., Furnival, J., Peter, E. and Donald. G. E., 1999, Pasture land cover in eastern Australia from NOAA-AVHRR NDVI and classified Landsat TM. *Remote sensing of environment.* 67, pp. 32–50.

Huete, A. R. 1988. A soil-adjusted vegetation index (SAVI). *Remote Sens. Environ*. 25, 295–309.

Jansa, J., 1998, A global topographic normalization algorithm for satellite images. *International Archives of Photogrammetry and Remote Sensing*. Vol. XXXII, Part 7, Budapest, pp. 8-15.

Jensen, J. R., 2000, An earth resource perspective. *Remote Sensing of the Environment.* 72, pp. 361-365.

Jones, A. R., Settle, J. J. and Wyatt, B. K., 1988, Use of digital terrain data in the interpretation of SPOT-1 HRV multispectral imagery. *Int. J. Remote Sensing*, Vol. 9, no. 4, pp. 669–682,

Ju, J., Gopal, T, S. and Kolaczyk, E. D., 2005, On the choice of spatial and categorical scale in remote sensing land cover classification. *Remote Sensing of Environment,* 96, pp. 62–77.

Kanellopoulos, I., Varfis, A., Wilkinson, G. G., and Megier, J., 1992, Land-cover discrimination in SPOT HRV imagery using an artificial neural network: a 20 class experiment. *International Journal of Remote Sensing*, 13, pp. 917-924.

Karoly, D. J., Braganza, K., Stott, P. A., Arblaster, J. M., Meehl, G. A., Broccoli, A. J. and Dixon, K. W., 2003, Detection of a human influence on north American climate**.** *Science*, Vol 302, pp. 1200-1203.

Kerr, J. T. and Cihlar, J., 2003, Land use and cover with intensity of agriculture for Canada from satellite and census data. *Global Ecology & Biogeography.* 12 , pp. 161–172.

Key, T., Warner, T. A., McGraw J. B. and Fajvan, M. A., 2001, A Comparison of multispectral and multitemporal information in high spatial resolution imagery for classification of individual tree species in a temperate hardwood forest. *Remote Sensing of Environment.* 75, pp. 112-121.

Kotschy, K.A., Rogers, K.H. and Carter, A.J., 2000, Patterns of change in reed cover and distribution in a seasonal riverine wetland in South Africa. *Folia Geobotanica*, 35, pp. 363-373.

Kremer, R. G. and Running, S. W., 1993, Community type data differentiation using NOAA/AVHRR data within a sagebrush-steppe ecosystem. *Remote Sens. Environ.,* 46, pp. :311–318.

Krumscheid, P., Stark, H. and Peintinger, M., 1998, Decline of reed at Lake Constance (Obersee) since 1967 based on interpretations of aerial photographs. *Aquatic Botany*, 35, pp.57-62.

Kulkarni, A. D., 1998, Neural-fuzzy models for multispectral image analysis. *Applied Intelligence,* 8, pp. 173–187.

LaFrance, J. T., Shimshack, J. P. and Wu, S. Y., 2002, The environmental impacts of subsidized crop insurance. *http://repositories.cdlib.org/are ucb/912R.*

Langley, S. K., Cheshire, H. M. and Humes, K. S., 2001, A comparison of single date and multitemporal satellite image classifications in a semi-arid grassland. *Journal of Arid Environments* 49, pp. 401-411.

Lass, L. W. and Thill, D. C., 2000, Detecting yellow starthistle (Centaurea solstitialis) with hyperspectral remote sensing technology. *Proc. West. Soc. Weed Sci*., 53, pp.11-22.

Lass, L. W., Prather, T. S. and Glenn, N. F., 2005, A review of remote sensing of invasive weeds and example of the early detection of spotted knapweed (Centaurea maculosa) and babysbreath (Gypsophila paniculata) with a hyperspectral sensor. *Weed Science,* 53, pp. 242–251.

Lass, L. W., Thill, D. C., Shafii, B. and Prather, T. S., 2002, Detecting spotted knapweed (Centaurea maculosa) with hyperspectral remote sensing technology, *Weed Technology*, 16, pp. 426– 432.

Lass, L. W. and Prather, T. S., 2004, Detecting brazilian pepper (Schinus terebinthifolius) with hyperspectral remote sensing technology. *Weed Technology*, 18, pp. 437– 442.

Lathrop R.G., Windham, L. and Montesano, P., 2003, Does Phragmites expansion alter

the structure and function of marsh landscapes? Patterns and processes revisited. *Estuarie*s, 26, pp. 423-435.

Latifovic, R., Zhu, Z., Cihlar, J., Giri, C. and Olthof, I., 2004, Land cover mapping of north and central America—global land cover 2000. *Remote Sensing of Environment,* 89, pp. 116–127.

Lauver, C. L. and Whistler, J. L., 1993, A hierarchical classification of Landsat TM imagery to identify natural grassland areas and rare species habitat. *Photogrammetric Engineering & Remote Sensing,* 59(5), pp. 627-634.

Lawrence, R. L., Wood, S. D. and Sheley, R. L., 2006, Mapping invasive plants using hyperspectral imagery and Breiman Cutler classifications (RandomForest). *Remote Sensing of Environmen*t, 100, pp. 356 – 362.

Liu, W.and Wu, E. Y., 2005, Comparison of non-linear mixture models: sub-pixel classification. *Remote Sensing of Environment,* 94, pp. 145–154.

Liu, Q.J., Takamiira, T., Takkuchi, N. and Shaao. G., 2002, Mapping of boreal vegetationof a temperate mountain in China by multitemporal Landsat TM imagery. *International Journal of Remote Sensing,* 23, pp. 3385-3405.

Lobo, A., Legenre, P., Rebollar, J., Carreras J. and Ninot, J., 2004, Land cover classification at a regional scale in Iberia: separability in a multi-temporal and multi-spectral data set of satellite images. *Int. J. Remote Sensing*, Vol. 25, No. 1, pp. 205–213.

Loveland, T. R. and Belward, A. 1997, The IGBP-DIS global 1 km land cover data set, DISCover first results. *Int. J. Remote Sensing*, Vol. 18, No. 15, pp. 3289–3295.

Malingreau, J. P., Achard, F., D'Souza, G., Stibig, H. J., D'Souza, J.,Estreguil, C. and Eva, H., 1995,. AVHRR for global tropical forest monitoring: the lessons of the TREES project. *Remote Sensing Reviews*, 12, pp. 29– 40.

Mayaux, P., Achard, F. and Malingreau, J. P., 1998, Global tropical forest area measurements derived from coarse resolution satellite imagery: a comparison

with other approaches. *Environmental Conservation,* 25, pp. 37– 52.

McIver, D.K. and Friedl, M.A., 2002, Using prior probabilities in decision-tree classification of remotely sensed data. *Remote Sensing of Environment,* 81, pp. 253– 261.

Michelson, D. B., Liljeberg, B. M. and Pilesjo, P., 2000, Comparison of algorithms for classifying Swedish land cover using Landsat TM and ERS-1 SAR data. *Remote Sensing of Environment*, 71, pp. 1 – 15.

Mundt, J., 2005, Discrimination of hoary cress and determination of its detection limits via hyperspectral image processing and accuracy assessment techniques. *Remote Sensing of Environment*, 96, pp. 509 – 517.

Mutanga, O. and Skidmore, A.K., 2004, Integrating imaging spectroscopy and neural networks to map grass quality in the Kruger National Park, South Africa. *Remote Sensing of Environment,* 90, pp. 104– 115.

Nowak, R. S. and Cdwell, M. M., 1999, Photosynthetic characteristics of crested wheatgrass and bluebunch wheatgrass. Journal of range management, 39(5), pp. 58-72.

O'Neill, A. L., 1996, Satellite-derived vegetation indices applied to semiarid shrublands in Australia. *Aust. Geogr.,* 27, pp. 185–199.

O'Neill, M. and Ustin, S. L., 2000, Mapping the distribution of leafy spurge at Theodore Roosevelt National Park using, AVIRIS. *Proceedings of the Ninth JPL Airborne Earth Science Workshop.*

Pareulo, J. M. and Lauenroth, W. K., 1995, Regional patterns of normalized difference vegetation index in north American shrublands and grasslands. *Ecology,* 76, pp. 1888–1898.

PCI, 2003, ANN parameters in EASI (Manual)

PFRA, 2001, PFRA generalized land cover report.

Peniuk, M., 1998, Revegetation of disturbed land with native species at Grasslands

National Park:1997 field trial. *Annual Report,* Vol. 4.

Peterson, D. L.and Price, K. P., 2002, Discriminating between cool season and warm season grassland cover types in northeastern Kansas. *Int. j. remote sensing,* Vol. 23, No. 23, pp. 5015–5030.

Peterson, E. B., 2005, Estimating cover of an invasive grass *(Brontus tectorum)* using tobit regression and phenology derived from two dates of Landsat ETM + data. *Iniemalional Journal of Remote Sensing,* Vol. 26, No. 12, pp. 2491-2507.

Qi, J., Chehbouni, A., Huete, A.R., Kerr, Y.H. and Sorooshian, S., 1994, A modified soil adjusted vegetation index. *Remote Sensing of Environment*, Vol. 48, pp. 119–126.

Qiu, F. and Jensen, J.R., 2004, Opening the black box of neural networks for remote sensing image classification. *International Journal of remote sensing,* Vol. 25 Issue 9, pp. 1749-1769.

Ramsey, R. D., Falconer, A. and Jensen, J. R., 1995, The relationship between NOAA-AVHRR NDVI and ecoregions in 37:547–562. *Remote Sens. Environ.,* 53, pp. 188–198.

Riano, D., Chuvieco, E., Salas, J. and Aguado I., 2003, Assessment of different topographic corrections in Landsat-TM data for mapping vegetation types. *IEEE Transactions on geoscience and remote sensing*, Vol. 41, No. 5, pp. 1056-1061.

Rice, D., Rooth, J. and Stevenson, J.C., 2000, Colonization and expansion of *Phragmites australis* in upper Chesapeake Bay tidal marshes. *Wetlands*, 20, pp. 280-299.

Rowley, R. J., 2002, Insuring the range: toward a crop insurance program for rangeland and pasture. [*Thesis for the degree of Master of Arts*].

Rowlinson, L.C., Summerton, M. and Ahmed, F., 1999, Comparison of remote sensing data sources and techniques for identifying and classifying alien invasive vegetation in riparian zones. *Water SA*, 25, pp. 497-500.

Sakamoto, T., Yokozawa, M., Toritani, H., Shibayama, M., Ishitsuka, N. and Ohno H., 2005, A crop phenology detection method using time-series MODIS data. *Remote Sensing of Environment*, 96, pp. 366 – 374.

Saltz, D., Schmidt, H., Rowen, M., Karnieli, A., Ward, D. and Schmidt, I., 1999, Assessing grazing impacts by remote sensing in hyper-arid environments. *Journal of range management,* 52(5), pp. 500-507.

Sandmeier, R. S. and Itten, K. I., 1997, A physically-based model to correct atmospheric and illumination effects in optical satellite data of rugged terrain. *IEEE Trans. Geosci. Remote Sensing,* Vol. 35, pp. 708–717.

Schmidt, H., 2002, Analysis of the temporal and spatial vegetation patterns in a semi-arid environment observed by NOAA AVHRR imagery and spectral ground measurements. *International journal of remote sensing,* Vol.23, No.19, pp. 3971-3990.

Soenen, S. A., Peddle, D. R. and Coburn, C. A., 2005, SCS+C: A modified sun-canopy-sensor topographic correction in forested terrain. *IEEE Transactions on geoscience and remote sensin*g, Vol. 43, No. 9, pp. 2148-2159.

Sommer, S., Hill, J. and Megier, J., 1998, The potential of remote sensing for monitoring rural land use changes and their effects on soil conditions. *Agriculture, Ecosystems and Environment*, 67, pp. 197–209.

Song, C. and Woodcock, C. E., 2003, Monitoring Forest Succession with multitemporal Landsat images: factors of uncertainty. *IEEE Transactions on geoscience and remote sensing*, Vol. 41, No. 11, pp. 1321-1330.

Stenberg, P., Rautiainen, M., Manninen, T., Voipio, P. and Smolander, H., 2004, Reduced simple ratio better than DVI for estimating LAI in Finnish pine and spruce stands. *Silva Fennica.* 38(1), pp 3–14.

Thomson, A. G. and Jones, C., 1990, Effects of topography on radiance from upland vegetation in North Wales. *Int. J. Remote Sens.*, Vol. 11, pp. 829–840.

Tian, Q. and Min. X., 1998, Vegetation index research progresses. *The geoscience to progress*, 13 (4), pp. 327- 333.

Tieszen, L. L., Reed, B. C., Bliss, N. B., Wylie, B. K. and DeJong, D. D., 1997, NDVI, C3 and C4 production, and distributions in Great Plains grassland land cover classes. *Ecol. Appl.,* 7, pp. 59–78.

Tokola, T., Sarkeala, J. and Linden, M. V., 2001, Use of topographic correction in Landsat TM-based forest interpretation in Nepal. *Int. J. Remote sensing*, Vol. 22, No. 4, pp. 551–563.

Tucker, C. J. and Townshend, J. R. G., 2000, Strategies for tropical forest deforestation assessment using satellite data. *International Journal of Remote Sensing*, 21, pp. 1461– 1472.

Warner, T. A., Lee, J. Y., and McGraw, J. B., 1999, Delineation and identification of individual trees in the Eastern, deciduous Forest. In *International Forum on Automated Interpretation of High Spatial Resolution Imagery for Forestry* (D. Hill and D. Leckie, Eds.), February 10–12, 1998, Victoria B.C., pp. 81–91.

Underwood, E., Ustin, S. and DiPietro, D., 2003, Mapping nonnative plants using hyperspectral imagery. *Remote Sensing of Environment,* 86, pp. 150–161.

USGS, 2003, Monitoring changes in vegetation and land surfaces by remote sensing—detecting infestations of cheatgrass on the Colorado Plateau. *http://climchange.cr.usgs.gov/info/sw/ monitor/remote1.html.*

Vieira, C. A. O. and Mather, P. M., 2000, A comparative study of multiple classifier combination methods in remote sensing. *Proceedings of the IC – Artificial Intelligence*, 1, pp. 39-45.

Vrindts, E., De Baerdemaeker, J. and Ramon, H., 2002, Weed detection using canopy reflection. *Precision Agriculture,* 3(1), pp. 63-80.

Warren, R.S., Fell, P.E., Grimsby, J.L., Buck, E.L., Rilling, G.C. and Fertik, R.A., 2001, Rates, patterns, and impacts of *Phragmites australis* expansion and effects of

experimental *Phragmites* control on vegetation, macroinvertebrates, and fish within tidelands of the lower Connecticut River. *Estuarie*s, 24, pp. 90-107.

Wessels, K.J., De Fries, R.S., Dempewolfa, J., Anderson, L.O., Hansen, A.J., Powell, S.L. and Moran E.F., 2004, Mapping regional land cover with MODIS data for biological conservation: examples from the Greater Yellowstone ecosystem, USA and Para´ State, Brazil. *Remote Sensing of Environment*, 92, pp 67–83.

Zhang, M., Liu, X. and O'Neill, M., 2002, Spectral discrimination of *Phytophthora infestants* infection on tomatoes based on principal component and cluster analyses, *Int. J. of RS,* 23(6), pp. 1095-1107.

Zhang, J., Rivard, B., Sánchez-Azofeifa, A. and Castro-Esau, K., 2006, Intra- and inter-class spectral variability of tropical tree species at La Selva, Costa Rica: Implications for species identification using HYDICE imagery. *Remote Sensing of Environment,* 105, pp. 129 – 141.

Appendix

Field data collection form

Topography	**Plot No.**										
	Slope										
	Aspect										
	Elevation										
	Lat.										
	Long.										
Cover-top layer	**Grass**										
	Forb										
	Shrub										
	Standing dead										
Cover-Low layer	**Litter**										
	Moss										
	Lichen										
	Rock										
	Bare ground										
Height	**Litter depth**										
	Average height										
Cover of grass species	**Needle & thread**										
	Western wheatgrass										
	Slender wheatgrass										
	Northern-wheatgrass										
	Blue gramma										
	June grass										
	Pasture sage										
	Sage brush										